© 2021. Published by The Company of Biologists Ltd | Development (2021) 148, dev199536. doi:10.1242/dev.199536

TECHNIQUES AND RESOURCES

RESEARCH ARTICLE

Identification of maternal-effect genes in zebrafish using maternal crispants

Cara E. Moravec, Gabriella C. Voit, Jarred Otterlee and Francisco Pelegri*

ABSTRACT

In animals, early development is dependent on a pool of maternal factors, both RNA and proteins, which are required for basic cellular processes and cell differentiation until zygotic genome activation. The role of the majority of these maternally expressed factors is not fully understood. By exploiting the biallelic editing ability of CRISPR-Cas9, we identify and characterize maternal-effect genes in a single generation, using a maternal crispant technique. We validated the ability to generate biallelic mutations in the germ line by creating maternal crispants that phenocopied previously characterized maternal-effect genes: *birc5b*, *tmi* and *mid1ip1*. Additionally, by targeting maternally expressed genes of unknown function in zebrafish, we identified two maternal-effect zebrafish genes, *kpna7* and *fhdc3*. The genetic identity of these maternal crispants was confirmed by sequencing haploid progeny from F0 females, which allowed the analysis of newly induced lesions in the maternal germ line. Our studies show that maternal crispants allow for the effective identification and primary characterization of maternal-effect genes in a single generation, facilitating the reverse genetics analysis of maternal factors that drive embryonic development.

KEY WORDS: Crispr, Maternal effect, Genome editing, Early development, Zebrafish, *Kpna7*, *Fhdc3*

INTRODUCTION

In zebrafish, the functions of many genes during development have been determined by inducing loss-of-function conditions through reverse genetic approaches. The establishment and advancement of targeted gene-editing technology, such as zinc-finger nucleases (ZFNs) (Doyon et al., 2008; Meng et al., 2008), transcription activator-like effector nucleases (TALENs) (Huang et al., 2011) and clusters of regularly interspaced short palindromic repeats (CRISPR) (Hwang et al., 2013), have led to the ability to create targeted genetic lesions in candidate genes. Previous work has shown that embryos injected with CRISPR-Cas9 have the potential to contain biallelic editing, which allows for the screening of embryonic phenotypes in somatic tissue of injected (F0) embryos, known as a 'crispant' (Burger et al., 2016; Jao et al., 2013; Shah et al., 2015; Shankaran et al., 2017; Trubiroha et al., 2018; Wu et al., 2018).

Early embryogenesis is dependent on a pool of maternal products, such as RNAs, proteins and other biomolecules, which drive developmental processes until zygotic genome activation (ZGA). Depletion of these maternal products, when essential, results in embryonic lethality. In animal species, mutations in maternally expressed genes disrupt early cellular processes, such as egg polarity and activation, pronuclear fusion, cytokinesis, cell adhesion, germ cell specification, and axis induction (Abrams and Mullins, 2009; Dosch, 2015). Maternally expressed genes can be robustly targeted with CRISPR-Cas9 (Campbell et al., 2015; Eno et al., 2016; He et al., 2018). However, an extra generation is necessary to observe maternal-effect phenotypes, which requires additional resources.

Here, we use maternal crispants to promote biallelic germline editing to achieve phenotyping of maternally expressed gene function in the next generation. We first validated this technique by using maternal crispants to phenocopy three known maternal-effect genes: *birc5b* (*motley*), *tmi* and *mid1ip1l* (*aura*) (Eno et al., 2016; Nair et al., 2013, 2021 preprint). Then, we selected four candidates with a potential maternal-only gene function by using the zebrafish genome assembly to identify multiple-copy gene families and stage-specific RNA-sequencing databases to predict maternal-specific expression. These candidates were tested for maternal-effect phenotypes using maternal crispants. Out of these four candidate genes, we identified two zebrafish maternal-effect genes, *kpna7* and *fhdc3*. Overall, these studies demonstrate the feasibility of using available databases coupled with a maternal crispant approach to identify and characterize, in a single generation, maternal-effect genes in zebrafish.

RESULTS

Workflow for germline crispant approach and maternal-effect phenotyping

A traditional workflow for generating a mutant zebrafish with CRISPR-Cas9 uses guide RNAs targeting a specific gene of interest, co-injected in F0 early embryos with Cas9 mRNA or Cas9 protein. Successful targeting generates stable lines for the identification of a recessive zygotic mutation in F3 embryos, a process that requires three generations (in zebrafish, approximately 9-12 months) from the time of injection. The identification of a mutation in a maternal-effect gene requires an additional generation to assess the phenotype in the progeny from a germ line with the loss-of-function condition (Fig. 1A).

Recent work has shown that the biallelic editing ability of CRISPR-Cas9 allows for the screening of zygotic phenotypes in somatic cells of embryos in the F0 generation, also known as 'crispants' (Burger et al., 2016; Jao et al., 2013; Shah et al., 2015; Shankaran et al., 2017; Trubiroha et al., 2018; Wu et al., 2018). Depending on the developmental process of interest, crispant embryos allow screening for the phenotype of targeted candidate genes in a few hours to a few days. In zebrafish, multiplexing guide RNAs to a single gene target has been shown to generate biallelic lesions with high efficiency (Wu et al., 2018). This increased efficiency should, in principle, allow the observation of maternal-effect phenotypes in the F1 generation in what we refer to as

Laboratory of Genetics, University of Wisconsin-Madison, WI 53706, USA.

*Author for correspondence (fjpelegri@wisc.edu)

C.E.M., 0000-0003-1670-6406; F.P., 0000-0002-0464-7042

Handling Editor: Steve Wilson
Received 19 February 2021; Accepted 19 August 2021

Development (2021) 148, dev199536. doi:10.1242/dev.199536

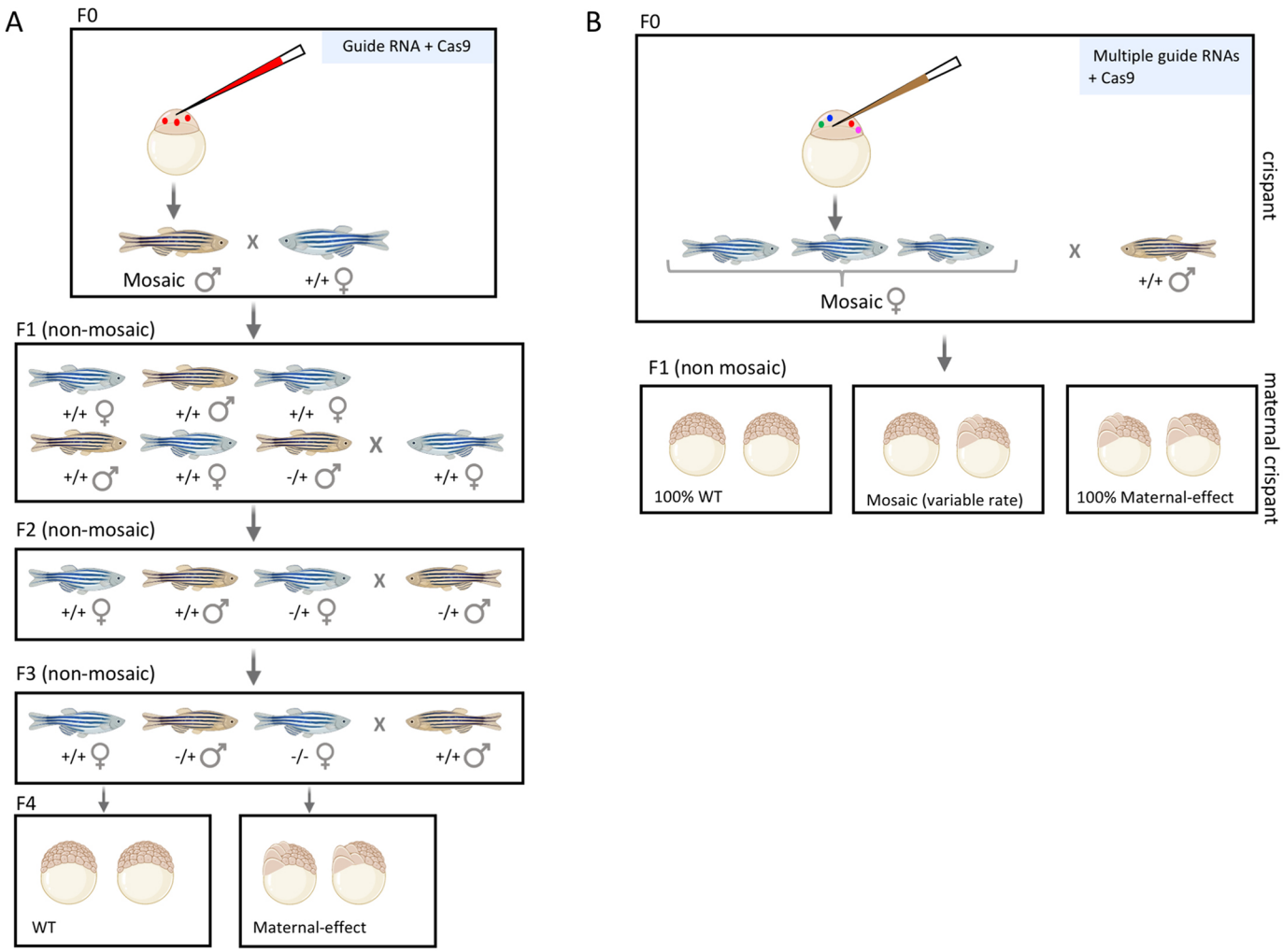

Fig. 1. Maternal crispants can be used to efficiently identify maternal-effect genes in zebrafish in a single generation. (A) The traditional workflow for CRISPR-Cas9 in zebrafish uses one guide RNA that is co-injected with Cas9 mRNA or protein into the one-cell embryo to target a specific gene of interest. Successful targeting will result in adults with a mosaic germ line. To isolate these alleles, non-mosaic F1 fish are generated by crossing the F0 CRISPR-injected fish with a wild-type fish, then screening for heterozygous carriers of indels. Outcrossing followed by incrossing results in female homozygous mutants for a maternal-effect gene, phenotypes of which can be assessed in their offspring. (B) The maternal crispant technique generates maternal-effect phenotypes in a single generation. This strategy multiplexes four guide RNAs to target a single gene, thus increasing the rate of biallelic editing. If this biallelic editing event occurs in the germ line, the F1 offspring of F0 CRISPR-injected females have the potential to display a maternal-effect phenotype.

'maternal crispant' embryos. The generation of maternal crispants would allow the phenotype of mutations in maternally expressed genes to be tested directly in the progeny of injected individuals.

For maternal crispants to occur, there must be biallelic editing events in cells fated to develop into the germ line. To generate maternal crispants with high efficiency, we designed four guide RNAs for each target, which included known or candidate maternal-effect genes. Guide RNAs were typically designed to target the first conserved domain of the protein, as listed on Ensembl, to increase the probability that any insertions or deletions (indels), both in-frame and out-frame shifts, abolish protein function. To generate maternal crispants, a cocktail containing multiplexed guide RNAs targeting a single gene and Cas9 protein was injected into one-cell (F0) embryos. Most embryos injected with the multiple guide RNA:Cas9 cocktail (>80%, compared with uninjected controls) were viable up to 5 days post-fertilization (dpf; Fig. S1). Once the injected F0 embryos reached adulthood, the resulting females (hereafter referred to as 'F0 females') were screened for maternal-effect phenotypes by scoring their offspring for developmental abnormalities (Fig. 1B). The resultant clutches from F0 females, presumably depending on the fraction of the germ line containing biallelic lesions, exhibited a range of phenotypes, from 0 to 100% affected embryos.

Validation of the maternal crispant approach using known maternal-effect genes

Three known maternal-effect genes, *birc5b*, *tmi* and *mid1ip1l*, which when mutated result in defects in cytokinesis in the early embryonic cell divisions (Eno et al., 2016; Nair et al., 2013, 2021 preprint), were chosen to validate the maternal crispant approach. Guide RNAs targeted the conserved regions for *birc5b* (BIR domain; Fig. 2A) and *tmi* (start of the MAP65/Ase/PRC1 domain; Fig. 2B), and the single exon for *mid1ip1l* (Fig. 2C). F0 females were mated to wild-type males, and the resulting F1 clutches were examined for phenotypes. In nearly all cases (9 of 10 F0 females), F1 clutches contained embryos with defects indistinguishable from those of embryos derived from females homozygous for the corresponding target gene (*birc5b*: 78-100%; *tmi*; 27-47%;

Development (2021) 148, dev199536. doi:10.1242/dev.199536

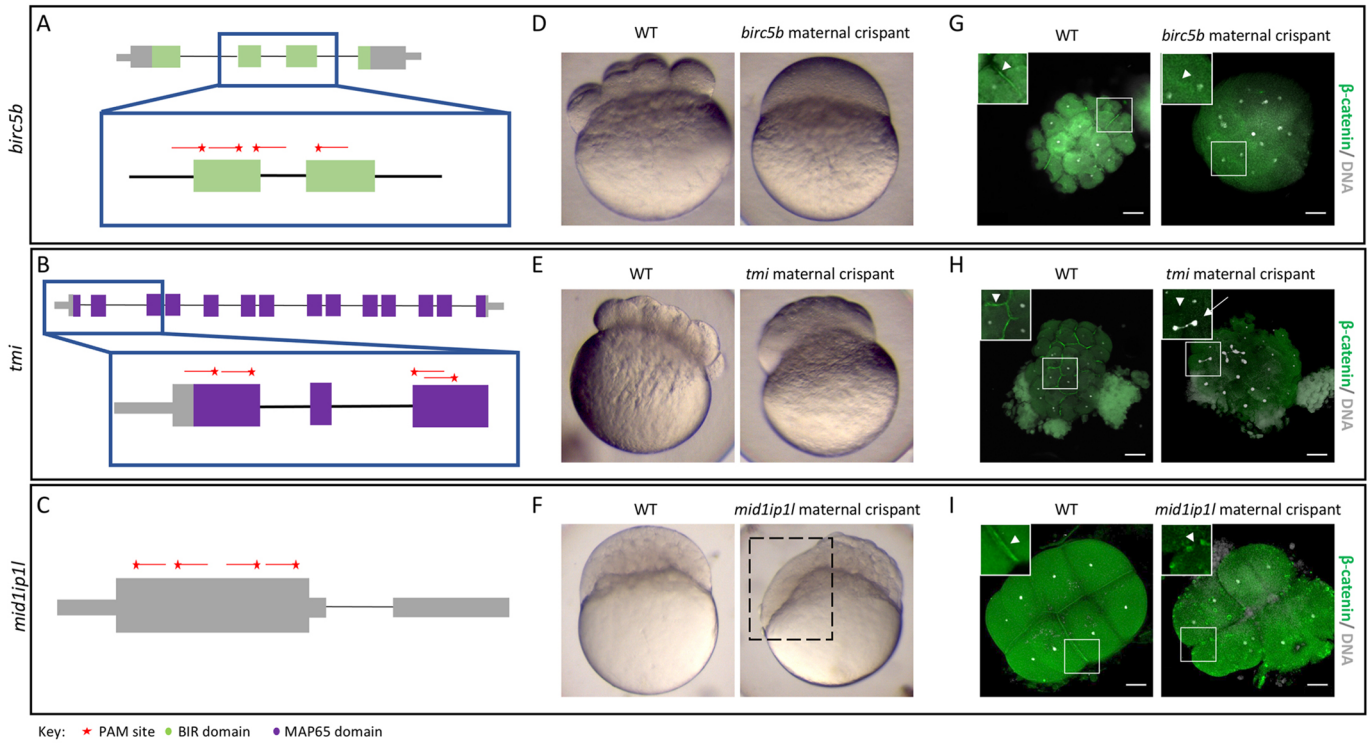

Fig. 2. Identification of known maternal-effect genes using maternal crispants. (A-I) Known maternal-effect phenotypes resulting from the mutagenesis of three genes, *birc5b* (A,D,G), *tmi* (B,E,H) and *mid1ip1l* (C,F,I), were replicated using the maternal crispant technique. (A-C) Gene structure diagrams of *birc5b* (A), *tmi* (B) *and mid1ip1l* (C) showing the target sites of guide RNAs (red lines) and PAM sites (red stars). (D-F) Representative comparisons of a live wild-type (WT) embryo with live time-matched maternal crispant embryos of *birc5b* [D; 75 min post-fertilization (mpf)], *tmi* (E; 75 mpf) and *midip1il* (F; 150 mpf), showing defects in cytokinesis identical to previous studies. The *mid1ip1l* maternal crispant embryo shown exhibits a partially syncytial phenotype (box in F). (G-I) Immunohistochemistry labeling of β-catenin and DAPI staining in *birc5b* (G; 90 mpf), *tmi* (H; 90 mpf) and *mid1ip1l* (I; 75 mpf) maternal crispants showing the lack of accumulation of β-catenin in mature furrows, confirming a failure in furrow formation in spite of DNA replication. *mid1ip1l* maternal crispants contain ectopic β-catenin-containing vesicles near the cortex. In all immunohistochemistry labeling, insets show high magnification images of the boxed areas, highlighting the differences in β-catenin localization (arrowheads) and asymmetric DNA segregation (arrow). Note that there is some embryo size variation caused by methanol storage of embryos. Scale bars: 100 µm.

mid1ip1l: 0-60%) (Table 1, Fig. S2). Two of the F0 females (for *birc5b*) produced 100% maternal crispant embryos, indicating that in these females most of, if not the entire, germ line contained biallelic edits. The remaining F0 females produced a fraction of embryos exhibiting the target mutant phenotype as well as wild-type embryos, reflecting a mosaic germ line. One F0 female (for *mid1ip1l*) did not yield maternal crispant embryos.

Characterization of the maternal crispants confirmed cellular defects identical to those caused by the loss of function of the corresponding target genes. Like embryos from *birc5b* homozygous females (Nair et al., 2013), *birc5b* maternal crispant embryos failed to create a visible furrow (Fig. 2D) and, despite normal DNA segregation, failed to accumulate the cell adhesion component β-catenin at furrow sites (Fig. 2G). Similar to embryos from females homozygous for *tmi* mutations (Nair et al., 2021 preprint), *tmi* maternal crispant embryos showed incipient cleavage furrows that underwent regression (Fig. 2E), and exhibited reduced β-catenin deposition at the furrow and aberrant chromosome segregation (Fig. 2H). Corresponding to embryos from females homozygous for *mid1ip1l* mutations (Eno et al., 2016), *mid1ip1l* maternal crispants exhibited abnormal cell division and became partially syncytial (Fig. 2F) with β-catenin present in unreleased cortical granules and unavailable for recruitment to the furrow (Fig. 2I).

In summary, for all three targeted known maternal-effect genes, a maternal crispant approach reliably replicates loss-of-function phenotypes.

Table 1. Fraction of embryos exhibiting a maternal crispant phenotype for targeted previously known maternal-effect genes, *birc5b*, *tmi* and *midlip1l*

Gene	Fish	Number of embryos in F1 generation	Phenotype (%)
birc5b	1	14	78
	2	145	100
	3	43	100
tmi	1	48	27
	2	82	47.5
	3	91	47.2
mid1ip1l	1	51	33.3
	2	82	60.9
	3	56	12.5
	4	30	0

Identification of maternal-effect genes via maternal crispants

The analysis of genes required for maternal functions is made difficult because of the requirement for additional generations to assess phenotypes in the offspring. In the case of maternal genes also required zygotically, the requirement for zygotic function also precludes the possibility of obtaining viable individuals to test maternal function. Maternal-specific genes typically have high transcript levels in the early embryo with a severe reduction in mRNA levels as the embryo undergoes ZGA (approximately 900

Development (2021) 148, dev199536. doi:10.1242/dev.199536

genes) (Aanes et al., 2011). In addition, a number of characterized maternal-effect mutations in zebrafish occur in genes that arose through gene duplication events, with the gene affected by the maternal-effect mutation expressed largely or exclusively maternally, and other copies, presumably the ancestral ones, retaining a more widespread function (Campbell et al., 2015; Eno et al., 2016; Ge et al., 2014; Nair et al., 2013, 2021 preprint). This pattern is consistent with the functional divergence of duplicated genes (Sandve et al., 2018), leading to some genes acquiring a maternal-only function. Thus, in these gene families, the zygotically expressed paralog(s) will perform essential functions in the somatic cells, thus permitting somatic development. In contrast, the maternally expressed duplicated paralog will only affect developing oocytes and progeny, allowing for the determination of its role in early development.

To identify candidates to target using a maternal crispant approach, we used an RNA-seq database that provides a baseline transcriptional profile for multiple developmental stages of the zebrafish, from zygote to 5 dpf (White et al., 2017). We searched for uncharacterized genes that: (1) displayed an expected profile for a maternal-specific gene, i.e. expressed in the oocyte and early embryo and degraded at ZGA, and (2) are gene duplicates for which one or more additional copies are expressed both maternally and zygotically, or zygotically only, reflecting a possible role for this second gene duplicate throughout development. These criteria are expected to enrich for maternally expressed gene duplicates for which knock out would have no effect on zygotic development in F0 fish but could lead to maternal-effect phenotypes. Using these criteria, we selected four candidate maternal-effect genes: *kpna7*, *fhdc3*, *zgc:114123* and *kcns3b*. These genes are predicted to carry out a diverse set of cellular functions in the zebrafish embryo, related to nuclear import (*kpna7*), regulation of actin dynamics (*fhdc3* and *zgc:114123*), and maintenance of cell membrane potential (*kcns3b*). The application of the maternal crispant technique to these genes allowed for the identification of maternal-effect phenotypes for two of these genes, *kpna7* and *fhdc3*. Targeting of *zgc:114123* and *kcns3b* led to clutches from F0 injected females that contained only phenotypically wild-type embryos (Table S1, Fig. S3), despite the production of multiple indels in F0 embryo somatic tissues 24 h after injection (Fig. S4).

Kpna7 is necessary for nuclear stability in the early embryo

In eukaryotic cells, large proteins are actively transported from the cytoplasm into the nucleus via a transport system mediated by a heterodimeric Importin α/β (also known as Karyopherin α/β) complex, which recognizes cargo containing a nuclear localization signal (NLS) (Conti et al., 1998; Görlich et al., 1994; Imamoto et al., 1995; Moroianu et al., 1995; Yasuhara et al., 2004).

Eukaryotes contain a varying number of Importin α genes. For example, yeast has a single Kpna gene, whereas mammals have seven Kpna genes (Hu et al., 2010; Kelley et al., 2010; Tejomurtula et al., 2009). Among mammalian Kpna genes, only *Kpna7* shows expression in the oocyte and the early embryo and RNA degradation at ZGA (Fig. 3A) (Boroviak et al., 2018; Hu et al., 2010; Tejomurtula et al., 2009; Wang et al., 2012). Similar to mammals, zebrafish also have seven Kpna genes (Fig. 3B), with *kpna7* exhibiting maternal-specific expression and transcript degradation at ZGA (Fig. 3B). Therefore, we targeted zebrafish *kpna7*, which has a canonical structure for this family of proteins composed of an N-terminal Importin-β binding domain and multiple armadillo repeats at the C terminus (Fig. 3C) (Conti et al., 1998; Görlich et al., 1994).

For the zebrafish *kpna7* maternal crispant, two guide RNAs were designed to target the Importin-β binding domain and two additional

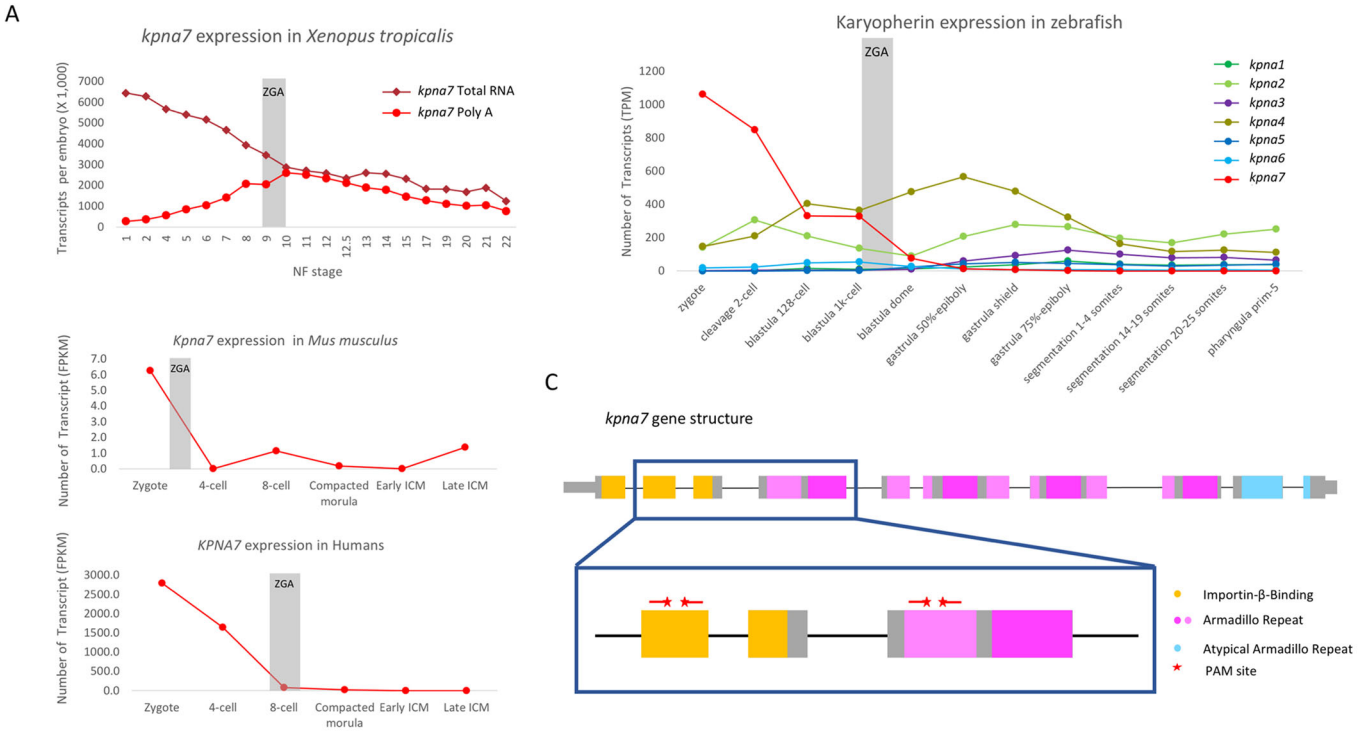

Fig. 3. Gene structure and expression of *kpna7* during development. (A) Expression levels of *kpna7* in other species display a similar pattern of the maternal expression of *kpna7* homologs. (B) Expression levels of the Kpna gene family throughout zebrafish development, from zygote to Prim-5 (24 hpf) stage. The maternal-specific transcript, *kpna7*, is represented in red and the gray bar marks the zygotic genome activation. (C) Diagram of the gene structure of *kpna7*, showing the known motifs and target sites of guide RNAs (red lines) and PAM sites (red stars).

Development (2021) 148, dev199536. doi:10.1242/dev.199536

Table 2. Fraction of embryos exhibiting a maternal crispant phenotype for candidate genes identified using gene expression and phylogenetic criteria, *kpna7* and *fhdc3*

Gene	Fish	Number of embryos in F1 generation	Phenotype (%)
fhdc3	WT	133	1.5
(yolk in blastodisc	1	43	74.4
at sphere)	2	51	100
	3	118	97.4
kpna7	WT	111	0
(stalled	1	40	100
development	2	25	100
at sphere)			

WT, wild type.

guide RNAs to target the first Armadillo repeat (Fig. 3C). Clutches from two different *kpna7* F0 females exhibited a maternal phenotype in 100% of the embryos (Table 2). During the cleavage stages, the *kpna7* maternal crispant embryos were morphologically indistinguishable from wild-type embryos. However, as they underwent development, the majority of these embryos stalled at sphere stage, with only a small fraction of embryos initiating epiboly and none completing this process (Fig. 4A). Labeling for β-catenin and DAPI at 6 h post-fertilization (hpf) showed that *kpna7* maternal crispant embryos exhibit an uneven distribution of nuclei, with a subset of cells appearing to lack DNA entirely (Fig. 4B, Movie 1) (n=15) and others exhibiting nuclei of a range of sizes and shapes, in contrast to their even distribution and size in wild type (Fig. 4B, Movie 1) (n=16).

In contrast to *kpna7* knockdown cancer cell lines, which exhibit supernumerary centrosomes (Vuorinen et al., 2018), all cells in *kpna7* maternal crispants showed the normal centrosome pair component (Fig. 4C; wild type: n=44 cells in 6 embryos; *kpna7* maternal crispants: n=39 cells in 7 embryos). However, *kpna7* maternal crispants exhibited defective DNA morphology in a majority of cells, reflected in nuclear material that failed to segregate to the spindle poles (Fig. 4C; wild type: 0/22 abnormal DNA segregation events in 6 embryos; *knpa7* maternal crispants: 17/21 abnormal DNA segregation events in 7 embryos). This defect, likely compounded through multiple rounds of cell division, presumably results in the uneven nuclear size and distribution observed at later stages. More comprehensive studies will be needed to study Kpna7 function in early development.

Fhdc3 is necessary for the yolk-blastodisc boundary function

Proteins of the Formin family are key regulators of cytoskeletal reorganization through the promotion of actin nucleation in the cell, with a well-established role in processes such as cytokinesis, cell polarization and filopodia assembly (Breitsprecher and Goode, 2013; Goode and Eck, 2007; Hegsted et al., 2017). A subset of proteins in the Formin family is known as 'inverted formins', in which the regulatory N-terminal region has been lost, leaving the FH1 and FH2 domains at the N-terminal region of the protein (Breitsprecher and Goode, 2013; Hegsted et al., 2017; Higgs and Peterson, 2005). Inverted formins have been shown to be involved in the linking of F-actin and microtubules and have a role in membrane trafficking and lumen formation (Breitsprecher and Goode, 2013; Hegsted et al., 2017; Higgs and Peterson, 2005; Young et al., 2008).

In zebrafish, the Fhdc family consists of five different genes: *fhdc1*, *fhdc2*, *fhdc3*, *fhdc4* and *fhdc5*; *fhdc3* is the only member with maternal-only expression and *fhdc5* is not expressed during the first 24 hpf (Fig. 5A). To generate *fhdc3* maternal crispants, guide RNAs were designed with one guide RNA targeting the protein before the FH1 domain and the other three guide RNAs targeting the start of the FH2 domain (Fig. 5B). Three *fhdc3* F0 females were screened, and all three generated clutches contained embryos exhibiting a consistent maternal-effect phenotype (Table 2). These embryos undergo normal cell cleavage during the first few cell cycles but, at approximately the 32-cell/64-cell stage, start to exhibit an aberrant constriction at the yolk-blastodisc boundary (Fig. 6A, black arrowhead). Immunolabeling of *fhdc3* maternal crispants with β-catenin and DAPI showed that at the 8-cell stage, the cellular layout (a 2×4 cell matrix at this stage) is similar between the *fhdc3* maternal crispants and stage-matched wild-type controls (Fig. 6C). However, at the 64-cell stage, when wild-type embryos exhibited a regular cellular layout (organized largely as two tiers of blastomeres, each in a 4×8 cell matrix), *fhdc3* maternal crispant embryos exhibited a disorganized cellular layout (Fig. 6C). The blastoderm of early

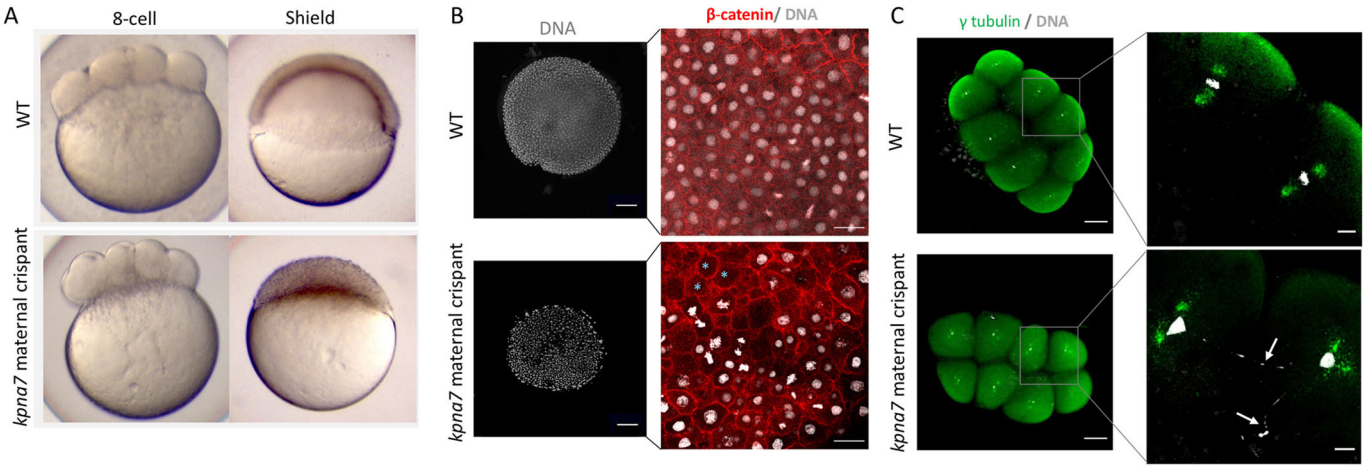

Fig. 4. Kpna7 is necessary for nuclear segregation during early development. (A) Images of live *kpna7* maternal crispant and wild-type (WT) controls at the 8-cell stage (75 mpf) and shield stage (6 hpf). At the 8-cell stage, *kpna7* maternal crispants appear to divide normally, but they stall at the sphere stage and fail to undergo epiboly. (B) Immunohistochemistry labeling of β-catenin and DAPI staining at 6 hpf showing that the *kpna7* maternal crispant embryos exhibit nuclei of unequal sizes, including a subset of cells that entirely lack nuclei (blue asterisks). (C) Immunohistochemistry labeling of γ-tubulin and DAPI staining at 75 mpf, showing that *kpna7* maternal crispant embryos display abnormal nuclear segregation (arrows) during cell cleavage. Scale bars: 100 µm (B,C, low magnification); 20 µm (B,C, high magnification).

Development (2021) 148, dev199536. doi:10.1242/dev.199536

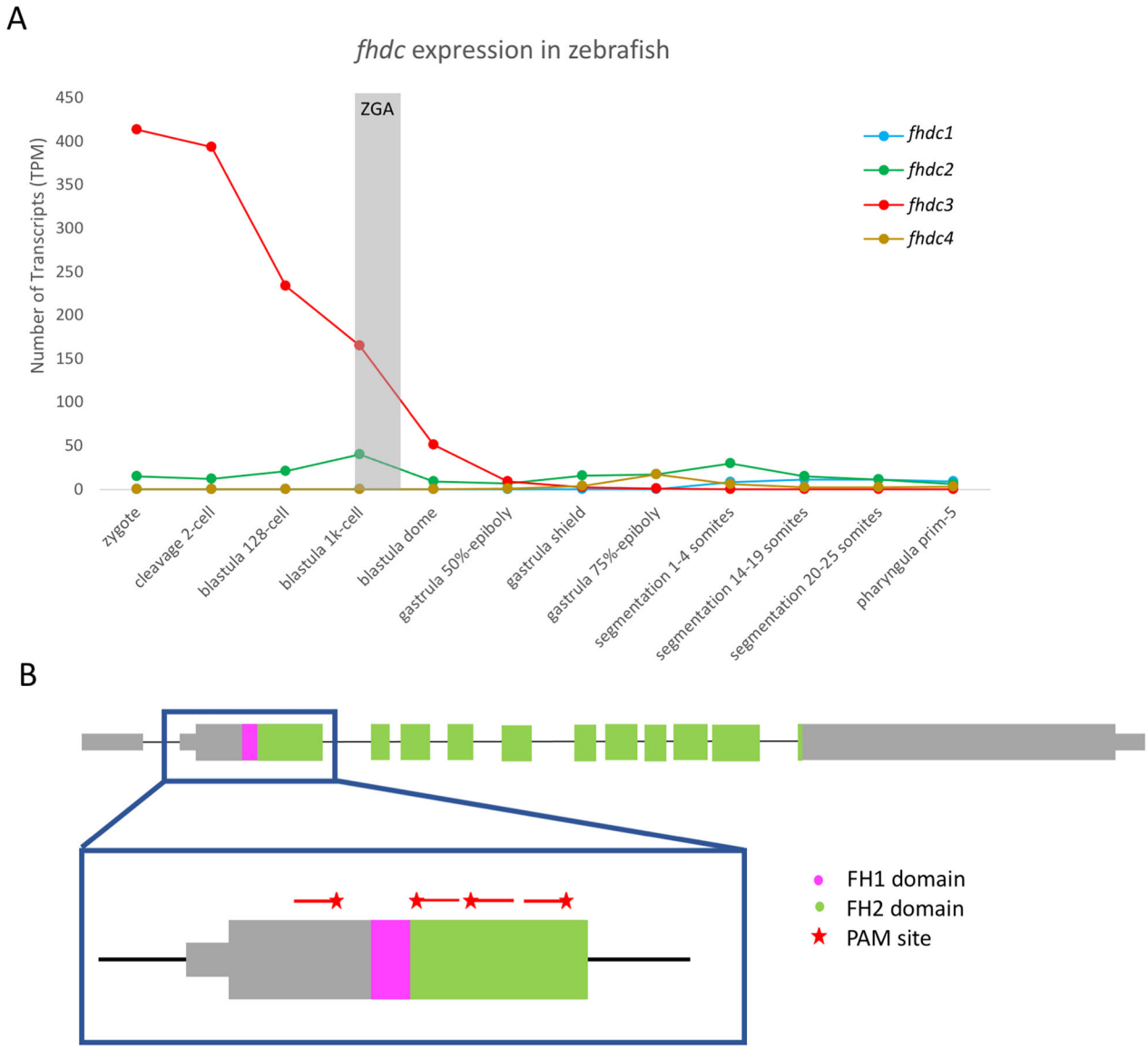

Fig. 5. Maternal expression and gene targeting of *fhdc3* during development. (A) Expression levels of the Fhdc gene family throughout zebrafish development, from zygote to Prim-5 (24 hpf) stage. The maternal-specific transcript, *fhdc3*, is represented in red and the gray bar marks the zygotic genome activation. (B) Diagram of the gene structure of *fhdc3*, showing the known motifs and target sites of guide RNAs (red lines) and PAM sites (red stars). Expression data from early development in other systems is not yet known.

wild-type embryos has an oblong shape (Kimmel et al., 1995), possibly caused by the coupling of blastomere division to spindle lengthening (Wühr et al., 2010; our own observations). Using a score of circularity (with a perfect circle having a score of 1) to assess blastoderm shape broadly, we found that, starting at the 64-cell stage, *fhdc3* maternal crispant embryos are significantly less oblong than wild type (Fig. 6D). Altogether, our observations indicate that embryos lacking *fhdc3* function are unable to maintain the ordered cellular arrangement of the early wild-type blastoderm.

Despite earlier defects, by late-cleavage stages *fhdc3* maternal crispants no longer showed an abnormal constriction of the yolk-blastoderm boundary phenotype, instead appearing at these stages, morphologically, relatively normal (Fig. 6A). Nevertheless, at these stages, *fhdc3* maternal crispant embryos contained presumptive ectopic yolk inclusions in varying numbers and sizes embedded in the blastodisc, presumably from a defective cytoplasm-yolk boundary at earlier stages (Fig. 6A). In addition, *fhdc3* embryos showed a consistent delay in the initiation epiboly (Fig. 6A), although embryos did not show yolk closure defects characteristic of previously described strong epiboly delayed mutant phenotypes (Kane et al., 1996) (Fig. 6B). Despite yolk inclusions and a delay in epiboly, *fhdc3* maternal crispants were able to proceed through gastrulation without apparent gross morphological defects up to 5 dpf (Fig. 6B, Fig. S5).

A closer examination of *fhdc3* maternal crispants at 24 hpf showed the continuing presence of presumptive ectopic yolk inclusions distributed in various regions of the embryo (Fig. 6B, black arrowheads, Fig. S5). *fhdc3* maternal crispant embryos that contained inclusions were significantly less likely than wild-type controls to be viable at 5 dpf, as assessed by swim bladder inflation (wild type: 96%, n=72; *fhdc3* maternal crispants: 39%, n=109; P=0.009) (Fig. S5).

The distinct aberrant constriction at the yolk-blastodisc boundary in *fhdc3* maternal crispants, and a predicted role for Fhdc3 as an

Development (2021) 148, dev199536. doi:10.1242/dev.199536

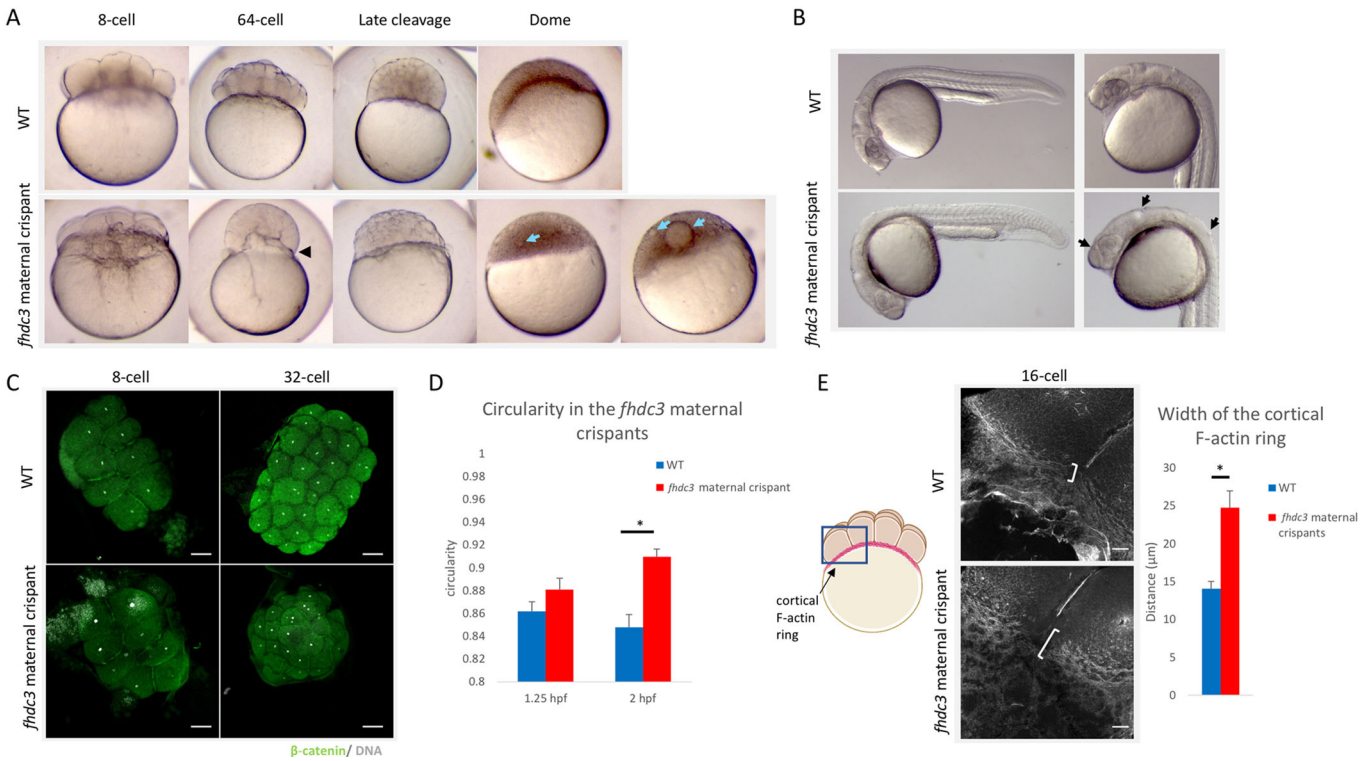

Fig. 6. Fhdc3 is necessary to maintain the yolk-blastodisc boundary during early development. (A) Images of live embryos comparing *fhdc3* maternal crispant embryos with time-matched wild-type (WT) controls during embryonic development. An abnormal constriction at the boundary between the blastodisc and yolk (black arrowhead) is observed during the early cleavage stages (64-cell). At later stages, a normal degree of constriction at the yolk-blastodisc boundary is restored, but embryos exhibit presumptive ectopic yolk inclusions (blue arrows). (B) At 1 dpf, *fhdc3* maternal crispant embryos do not exhibit gross morphological defects, although they still contain presumptive ectopic yolk inclusions (arrows). (C) Immunolabeling of β-catenin and DAPI staining at 8-cell and 64-cell stages, showing that the overall shape and cell organization of the embryo are affected in the later *fhdc3* maternal crispant embryos. (D) At the 8-cell stage, there is no significant difference in the shape of wild-type and *fhdc3* maternal crispant embryos [*fhdc3* maternal crispant score of circularity 0.881 (n=18); wild type 0.8615 (n=13); P=0.0893] but the shape appears significantly different at the 64-cell stage [*fhdc3* maternal crispants: 0.90963 (n=8), wild type: 0.84757 (n=7); P=0.0003]. Error bars represent s.e.m. (E) At the 16-cell stage, the cortical F-actin ring appears significantly wider in the *fhdc3* maternal crispant [*fhdc3* maternal crispants: 24.8 µm (n=10), wild type: 14.1 µm (n=10); P=0.0003]. Error bars represent s.e.m. Brackets indicate the width of the cortical F-actin ring at the location shown in the schematic. Scale bars: 100 µm (C); 20 µm (E).

actin regulator, led us to analyze the cortical F-actin ring in *fhdc3* maternal crispant embryos. Visualization of the yolk-blastodisc boundary of 16-cell embryos with rhodamine-conjugated phalloidin showed that the cortical F-actin ring in *fhdc3* maternal crispant is wider compared with time-matched wild-type controls (*fhdc3* maternal crispants: 24.8 µm, n=10; wild type: 14.1 µm, n=10; P=0.0003) (Fig. 6E).

Our observations suggest that *fhdc3* plays an essential role in regulating the yolk-blastodisc boundary in the early embryo, and is required for segregation of the yolk away from the blastodisc and, eventually, embryonic survival.

Identification of genetic lesions in maternal crispants

The multiple populations of alleles in traditional crispants, which typically occur in diploid cells and involve a mixture of induced lesions, can lead to challenges in interpreting the sequences of targeted genes. To facilitate the analysis of lesions in maternal crispants, we took advantage of the ability to generate haploid embryos in zebrafish (Walker, 1998) and sequenced alleles present in single haploid maternal crispant embryos. This combined approach allowed for straightforward identification and characterization of genetic changes to the target sites by Sanger sequencing (Fig. 7).

We identified genetic lesions in single maternal crispant haploid embryos from *birc5b*, *tmi*, *kpna7* and *fhdc3* maternal crispants. *mid1ip1l* maternal crispant embryos had a fragile cortex, as previously shown in embryos from females homozygous for the *mid1ip1l* mutation (Eno et al., 2016), did not survive the manipulation and were excluded from the analysis. All generated maternal crispant haploid embryos were sequenced (3-13 embryos per female, see Materials and Methods). Every sequenced maternal crispant haploid contained genetic lesions in the expected targeted gene, consistent with the germ line containing biallelic mutations in those targets (Figs 8 and 9, Table 3).

In traditional zygotic crispants, it has been reported that the injected embryos are mosaic and contain multiple alleles, a majority of which are frameshifts leading to premature stop codons (Trubiroha et al., 2018; Wu et al., 2018). In these zygotic crispants, when multiple guide RNAs are used, mutations are observed in all four guide sites at varying frequencies, with some lesions being larger deletions spanning multiple guide sites (Wu et al., 2018). Similar to traditional crispants, edited lesions in maternal crispants included mutations in multiple guide sites as well as site-spanning deletions, with a majority of DNA lesions containing frameshifts and premature stop codons (Figs 8 and 9, Table 3). We found that maternal crispant embryos exhibit lesions in only a subset of the guide sites (Table 3), with the same guide sites being edited in different F0 females (Figs 8 and 9). For example, *birc5b* maternal crispants from three different F0 females contained

Development (2021) 148, dev199536. doi:10.1242/dev.199536

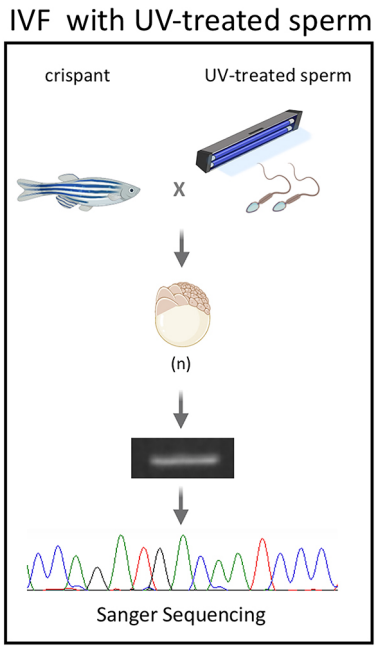

Fig. 7. Indels can be identified in maternal crispants by producing haploids. IVF of crispant oocytes with UV-treated sperm generates embryos with a single maternal allele, facilitating Sanger sequencing and genetic analysis.

mutations only in guide sites three and four, and *fhdc3* maternal crispants from three different F0 females only in guide site four (Figs 8 and 9, Table 3). This is consistent with previous studies demonstrating that selective site usage and repair are influenced by the cellular environment (Allen et al., 2018).

Collectively, DNA lesions observed in the set of individually analyzed haploid maternal crispants represent the mixture of induced alleles present in the germ line, either in different germ cells or in either of the two different gene copies present in diploid, pre-meiotic germline cells. Thus, sampling of targeted lesions in maternal crispants is expected to reveal multiple lesions, reflecting both the mosaicism and diploid content of the maternal germ line. Consistent with this expected complexity, we observed up to four different alleles in clutches of maternal crispant embryos from single F0 females, with an average of approximately two alleles per clutch. Assuming random segregation, each of the two maternal alleles in germline cells containing biallelic lesions is expected to be transmitted to maternal crispants in an approximately 1:1 ratio. Interestingly, lesions identified in single maternal crispants haploids were not recovered in such equal ratios. For example, of ten haploid maternal crispant embryos sequenced from *tmi* crispant fish two, all had an identical allele (Fig. 9A). This unexpected uneven recovery of germline lesions could reflect a biased repair mechanism of CRISPR-Cas9-induced lesions in the germ line, as observed in other systems (Allen et al., 2018; Brunner et al., 2019).

In summary, we identified genetic lesions in targeted maternal genes in all analyzed haploid embryos from F0 females, consistent with maternal crispant progeny embryos being derived from germ cells with biallelic lesions in those gene targets.

Establishment of a stable line to confirm a maternal crispant phenotype

Confirmation that observed maternal crispant phenotypes correspond to the targeted genes requires the analysis of the phenotype in stable CRISPR-Cas9 mutant lines, an approach that we carried out for *kpna7*. We outcrossed an F0 male sibling of an F0 female that yielded maternal crispant embryos to propagate a CRISPR-Cas9 edited allele, *kpna7*^{uw107}. This allele contains two mutations in the *kpna7* gene, one in guide site three (6 bp deletion) and one in guide site four (11 bp deletion) (Fig. S6A), with the second mutation creating a premature stop codon (Fig. S6B). As expected, homozygous mutant females for *kpna7*^{uw107} led to a 100% phenotype in progeny embryos similar to that of *kpna7* maternal crispants: most embryos stalled at the sphere stage (Fig. S6C), with only a fraction of the embryos initiating epiboly

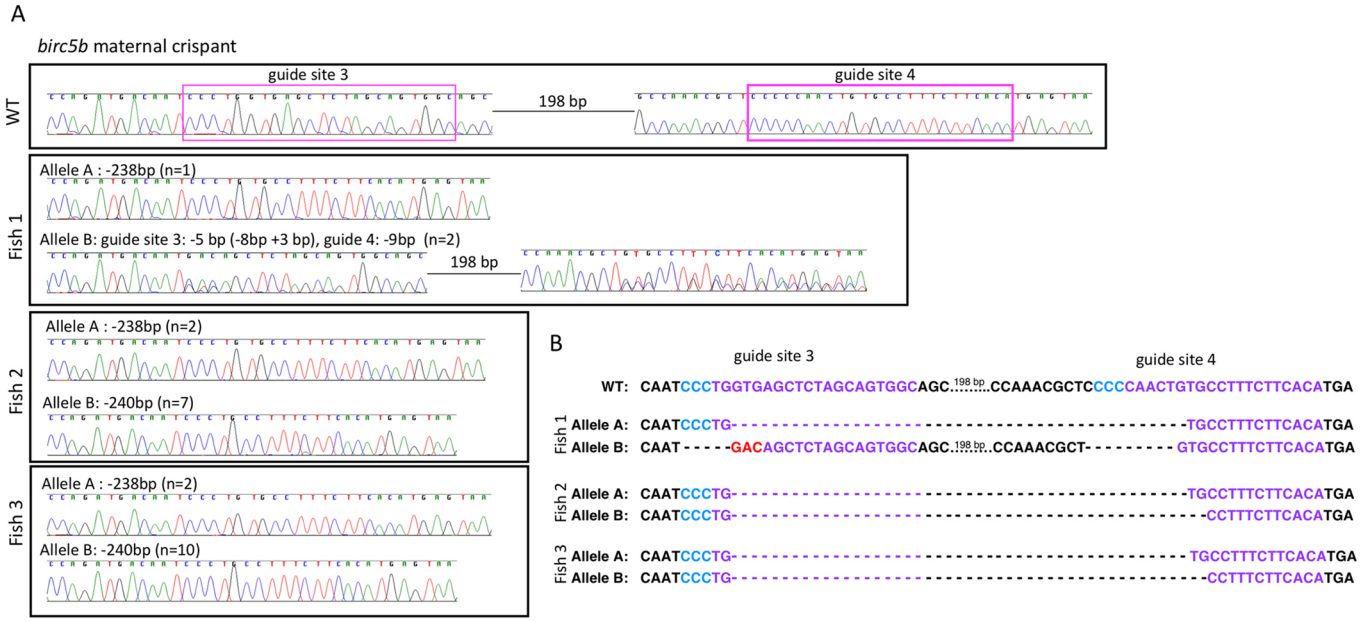

Fig. 8. Sequencing data from haploid *birc5b* maternal crispants. (A) Chromatograms of sequences for guide sites that contained indels after CRISPR-Cas9 mutagenesis in a wild-type (WT) embryo and *birc5b* maternal crispant haploids from three different F0 fish. (B) Alignment of sequences corresponding to the chromatograms, with the guide sites in purple and the PAM sites in blue. Red text indicates the addition of new base pairs and dashes deleted bases.

Development (2021) 148, dev199536. doi:10.1242/dev.199536

Fig. 9. Sequencing data from maternal crispant haploids for *tmi*, *kpna7* and *fhdc3* showing the generated lesions. (A-C) Alignment of sequences for *tmi* (A), *kpna7* (B) and *fhdc3* (C) maternal crispants with the guide sites in purple and the PAM sites in blue. Red text indicates the addition of new base pairs and dashes deleted bases.

and all embryos lysing prior to 24 hpf (n=365 embryos). The phenotype of embryos from non-mosaic *kpna7*^{uw107} homozygous females confirms the target in the corresponding maternal crispants and provides proof of principle for the use of maternal crispants to identify maternal-effect genes.

DISCUSSION

In this study, we developed a reverse genetic approach to identify, in a single generation, maternal-effect genes required for early embryonic development of the zebrafish. The maternal crispant strategy described in this paper utilizes the biallelic editing abilities of CRISPR-Cas9 through multiplexing of guide RNAs (Burger et al., 2016; Jao et al., 2013; Shah et al., 2015; Shankaran et al., 2017; Trubiroha et al., 2018; Wu et al., 2018) to identify maternal-effect genes in a resource-efficient manner. As a proof of principle for the maternal crispant approach, we recovered maternal crispant embryos for five out of the seven genes tested. Furthermore, the combination of maternal haploids and Sanger sequencing allowed us to identify and characterize indels in maternal crispants, facilitating the association of observable phenotypes to the gene targets. We additionally validated the *kpna7* maternal crispant phenotype using an established stable line. Thus, our studies show that the production of maternal crispants is an effective strategy for identification of maternal-effect genes.

A maternal crispant approach allows the direct generation of maternal-effect phenotypes

Using a maternal crispant approach, we were able to identify maternal-effect phenotypes reliably. In experiments targeting the five

Table 3. Percentage induction, location and type of indels found in four of the maternal crispants

	birc5b	*tmi*	*kpna7*	*fhdc3*
Number of F0-injected females used	3	2	2	3
Total number of embryos sequenced	24	18	19	32
Total number of embryos with indels	24	18	19	32
Mutation in one site	0	0	13	32
Mutations in multiple sites	24	18	6	0
Location of indels				
Guide site 1	0	0	0	0
Guide site 2	0	18	0	0
Guide site 3	24	18	19	0
Guide site 4	24	10	6	32
Types of indels				
In-frame mutation	5	17	6	1
Frame-shift mutation	21	19	19	31
Average predicted protein length for maternal crispant alleles	WT: 144 AA Maternal crispant: 95 AA	WT: 508 AA Maternal crispant: 189 AA	WT: 520 AA Maternal crispant: 127 AA	WT: 806 AA Maternal crispant: 131 AA

AA, amino acid; WT, wild type.

Development (2021) 148, dev199536. doi:10.1242/dev.199536

genes for which maternal crispant phenotypes were observed, most (14/15) screened F0 females produced embryos that showed maternal-effect phenotypes. The clutches recovered from F0 females contained on average 69% maternal crispant embryos. The combination of these results suggests efficient biallelic editing of the germ line for multiple targets, thus allowing for the identification of maternal-effect phenotypes in the progeny of injected (F0) fish.

Other advantages of the maternal crispant screen are that the clutches can contain an internal control, and it is straightforward to establish stable mutant lines. The mosaic clutches that occur when phenotypically wild-type embryos are derived from oocytes without biallelic genetic edits in a mosaic F0 germ line can act as an internal control for variables such as fertilization time and developmental rate. This method also allows the simultaneous establishment of stable mutant lines, either from F0 sibling males, as demonstrated with the *kpna7*^{uw107} allele, or from F1 offspring carrying induced lesions. These stable lines can be used to confirm phenotypes observed in the maternal crispants.

In these studies, we only identified maternal-effect phenotypes from gross morphological defects, and this approach may identify a large fraction of maternal-effect mutations. However, lethality might not be a necessary outcome for a maternal-effect phenotype. For example, depletion of Rest (NRSF) in zebrafish embryos causes the upregulation of target genes leading to changes in primary motor neuron architecture and behavior (Moravec et al., 2016). The use of transgenic lines that highlight specific structures or cell types, as has been done for heart and thyroid development in zygotic crispants (Trubiroha et al., 2018; Wu et al., 2018), would further increase the power of the approach. This maternal crispant technique also has the potential to determine the maternal function of genes required both maternally and zygotically, by specifically targeting Cas9 activity to the germ line (Moreno-Mateos et al., 2015).

Genetic variation in maternal crispants

A survey of haploid maternal crispants showed that genetic lesions tended to involve certain guide sites but not others. In some cases, multiple independently created lesions involving identical improperly repaired sequences were found in the progeny of different F0 females. This apparent guide site selectivity contributed to limited genetic variation in maternal crispants for specific genes.

Interestingly, we found that a majority of edited alleles are not recovered equally in maternal crispants of the same clutch. For example, in the case of *tmi*, ratios of recovery of two different alleles in haploid embryos were 7:1 (female 1) and 10:0 (female 2). Depending on the time of the edit, different numbers of germ cells will carry newly induced alleles, thus influencing the ratio of alleles present in the germ line. The uneven recovery of alleles could be caused by a repair confirmation bias for specific indels (Allen et al., 2018), resulting in identical independent edits in one or more germline cells. Another possibility is that a double-stranded break in one chromatid is corrected using an edited sister chromatid as a template, through homologous recombination/homology-directed repair (Brunner et al., 2019), creating identical mutations in both copies of the gene in the same germline cell. We cannot rule out an alternative explanation whereby the observed uneven allele recovery is caused by biased segregation during meiosis, possibly caused by damage to one chromatid.

Selection of maternal-effect candidate genes using bioinformatic approaches

We identified genes that are likely candidates to have a maternal-effect function using a combination of an RNA-sequencing database (White et al., 2017) and phylogenetic analysis. In eukaryotes, whole-gene duplications have allowed significant evolutionary events to occur because the functions of the duplicated genes are less constrained (Long et al., 2003; Lynch and Conery, 2000; Ohno, 2013). In these cases, one of the gene copies can provide an essential basic function, allowing a second gene copy to acquire new functions. The zebrafish genome has undergone multiple rounds of whole-genome duplications (Meyer and Schartl, 1999), with a portion of duplicated genes experiencing functional divergence to develop new roles, including a maternal-specific function. Bioinformatic analysis has determined that the zebrafish genome has 3991 duplicated sets of genes (Lu et al., 2012). A rough estimate suggests that out of the approximately 900 maternally expressed genes there may be over 100 genes that additionally belong to families of gene paralogs that can be tested with this approach. Our studies are consistent with this phenomenon and suggest that a combination of expression data coupled to phylogenetic analysis allows for the effective identification of gene candidates with maternal-specific functions.

Identification of maternal-effect genes in early development

Using the above criteria, we selected four candidate maternal genes and tested their function using a maternal crispant approach. Out of these four genes, we identified maternal-effect phenotypes in two of the genes, *kpna7* and *fhdc3*.

Past research in mice has shown that loss-of-function conditions for *kpna7*, an Importin α involved in nuclear transport, results in imbalanced sex ratios, with mutant females producing embryos with an embryonic-lethal phenotype (Hu et al., 2010). Knockdown of this maternally expressed transcript in other mammalian embryos, i.e. cattle and pigs, also showed reduced cellular cleavages leading to arrested embryonic development, similar to the 100% maternal-effect lethal phenotype that is observed in zebrafish (Tejomurtula et al., 2009; Wang et al., 2012). This developmental stall in zebrafish is likely due at least partly to the elimination of nuclei from a subset of cells during development, which precludes zygotic genome activation and epibolic movements in those cells (Kane et al., 1996; Knaut et al., 2000; Lee et al., 2013; Lindeman and Pelegri, 2012). The *kpna7* maternal crispant suggests a link between Kpna7 function in nuclear import and DNA segregation.

A second maternal crispant target in this study was *fhdc3*, a maternally expressed homolog of the inverted formin *fhdc1*. *fhdc3* maternal crispants exhibit an exaggerated constriction of the cytokinetic ring. In wild type, this actin-based ring forms at the margin of the blastodisc during the early cleavage stages and is thought to drive ooplasmic flow and yolk segregation during cycles of contraction and relaxation associated with the cell cycle (Fuentes and Fernández, 2010; Leung et al., 2000). The exaggerated constriction phenotype in *fhdc3* maternal crispants is no longer observed after the 6th cell cycle, a time coincident with the disappearance of the cytokinetic ring in wild type. However, *fhdc3* crispant embryos continue to exhibit defects as reflected by presumptive ectopic yolk inclusions in the embryo proper and reduced embryonic viability. Thus, *fhdc3* is a maternal gene with a temporarily restricted yet essential function in regulating the F-actin-based cytokinetic ring during the earliest embryonic cell cycles, which contributes to proper segregation of yolk from the cytoplasm.

We did not identify maternal-effect phenotypes for two targeted genes, the Spire family gene *zgc:114123* and the S subfamily potassium channel *kcns3b*, despite efficient production of indels in somatic cells of injected F0 embryos. Considering the expression

Development (2021) 148, dev199536. doi:10.1242/dev.199536

pattern of *zgc:114123* and the role of Spire in oogenesis in other systems (Bradley et al., 2020; Leader et al., 2002; Manseau and Schüpbach, 1989; Pfender et al., 2011), it is possible that a loss of function for *zgc:114123* affects oocyte development, precluding the production of maternal crispant embryos in F1 clutches. The number of maternal transcripts for *kcns3b* is significantly lower than other targets in our studies, so that the absence of maternal crispants for this gene may reflect a minor or non-essential role for this gene during development.

In summary, this study presents an effective approach for producing embryos with loss of function for maternal-effect genes, taking advantage of a high rate of CRISPR-Cas9-induced biallelic editing in the germ line. The resulting maternal crispants allow for the identification and characterization of maternal-effect genes in a single generation. In teleost fish, a subset of maternal genes has arisen from gene duplication events, and targeting maternal-specific duplicate genes could provide insight into the role of gene homologs in development and evolution. Thus, a maternal crispants approach could help to expedite our understanding of the role of maternal products during development.

MATERIALS AND METHODS

Animal husbandry

Stocks of wild-type AB or crispant fish were raised and maintained under standard conditions at 28.5°C (Brand et al., 2002). Embryos were collected by natural matings and allowed to develop in E3 embryonic medium (Brand et al., 2002), with staging according to age and morphological standards (Kimmel et al., 1995). All zebrafish housing and experiments were approved by the University of Wisconsin-Madison Institutional Animal Care and Use Committee.

Guide RNA design and synthesis

The CRISPR design web tool CHOPCHOP was used to identify guide RNA sites with high activity and minimal predicted off-target sites (Labun et al., 2016; Montague et al., 2014; Moravec and Pelegri, 2019). Four guide RNAs were selected for each target gene with the following criteria: predicted to have high cleaving activity; located in or near the first predicted protein domain (as identified by Ensembl; Aken et al., 2016); and minimal to no overlapping regions between guide RNAs.

Guide RNA templates were produced using an annealing/fill-in method as described (Gagnon et al., 2014). Briefly, guide RNA templates were generated with a gene-specific oligo containing an SP6 promoter sequence, a gene-specific target sequence, and an overlapping sequence complementary to the constant oligo (Table S2). Annealing/fill-in was performed using T4 DNA polymerase using 100 µM of each of the oligo fragments. Oligos for each of the four gene-specific guide RNAs were separately annealed to the constant oligo. After the T4 DNA polymerase fill-in, the four guide RNA templates were pooled together and concentrated by purification using a DNA Clean and Concentrator kit (Zymo Research).

A pooled guide RNA cocktail was synthesized using the MEGAshortscript T7 Transcription Kit (Invitrogen) using the concentrated pooled guide RNA template. After RNA synthesis, the guide RNA pool was purified using an ethanol/ammonium acetate protocol. The concentration of the guide RNA pool was measured by a NanoDrop ND-2000 spectrophotometer, and its integrity was checked by gel electrophoresis. Single-use aliquots of guide RNAs were stored at −80°C.

Guide RNA/Cas9 injection

A mixture of the pooled guide RNA cocktail (200 pg/nl total final concentration) and Cas9 protein (PNA Bio; 400 pg/nl final concentration) was injected into one-cell-stage AB embryos. At 24 hpf, a subset of the injected embryos was collected, and DNA was extracted as previously described (Meeker et al., 2007). Guide activity was assayed by amplifying 120-100 bp fragment across the target site via PCR (Table S2) and then resolved on a 2.5% agarose gel. If Cas9-mediated genetic edits were created in the somatic cells, a population of DNA that contains a variety of indels would generate a smear, confirming Cas9 activity (Moravec and Pelegri, 2019).

Phenotypic analysis of maternal crispant embryos

Injected embryos were raised until sexual maturity, and then all F0 females were mated through natural crosses to AB males. F1 embryos were collected approximately every 15 min and were allowed to develop in 100-mm Petri dishes with 1× embryonic medium (E3); each 100 mm-diameter dish contained no more than 100 embryos to ensure proper medium oxygenation. Control synchronized wild-type embryos and phenotypically wild-type embryos present in the F1 clutches were used to determine time from fertilization. Development was monitored in live embryos every hour for the first 8-10 h, at 24 hpf, and twice a day thereafter until 5 dpf. Maternal crispants were scored for possible gross morphological defects, such as defective cellular division, deviations from the wild-type body plan, developmental delays, and failure to develop a swim bladder. For documentation of maternal-effect phenotypes, embryos younger than 24 hpf were left in their chorions and imaged on glass-bottom dishes containing 1× E3, and embryos older than 24 hpf were dechorionated and imaged on glass-bottom dishes containing 3% methylcellulose. All live images were acquired using a Leica MZ FLIII microscope equipped with a Leica EC3 camera and Leica Acquire version 1.0 RC4 software.

Immunofluorescence and microscopy

Embryos were fixed in 4% paraformaldehyde in PBS and immunolabeled as previously described (Lindeman and Pelegri, 2012), with antibody incubation overnight at 4°C. Primary antibodies were rabbit anti-β-catenin (1:1000, Sigma-Aldrich, C2206), mouse anti-β-catenin (1:1000, Sigma-Aldrich, C7207) and mouse anti-γ-tubulin (1:2000, Sigma-Aldrich, T6557). Secondary antibodies were goat anti-rabbit IgG, Alexa 488 (Molecular Probes, A-11008), goat anti-rabbit IgG, Cy3 (Jackson ImmunoResearch, 111-165-144), rabbit anti-mouse, Alexa 488 (Molecular Probes, A-11059) and goat anti-mouse IgM, Cy3 (Jackson ImmunoResearch, 115-165-062). Actin was labeled as previously described (Eno and Pelegri, 2018) with rhodamine-conjugated phalloidin. To detect DNA, embryos were labeled with a 0.5 µg/ml solution of 4′,6-diamidino-2-phenylindole-dihydrochloride (DAPI) for 10 min followed by three washes in PBS. After labeling, depending on imaging conditions, embryos were either directly mounted sideways on the slide or deyolked and mounted flat with the animal pole upwards, in both cases in 75% glycerol. Images were obtained using a Zeiss LSM780 confocal microscope and analyzed using ImageJ.

Analysis of *fhdc3* maternal crispants

To examine the shape of the early *fhdc3* and wild-type embryos, traces of the perimeters of embryos at 1.25 and 2 hpf were analyzed using ImageJ. Embryos with presumptive ectopic yolk inclusions were classified as having either small or large inclusions (less than or more than one-eighth of the blastodisc volume, respectively) by estimating the volume of the largest yolk inclusion in the blastodisc at sphere stage and, together with AB wild-type controls, were grown individually in 24-well tissue culture dishes containing 1-1.5 ml of E3 for 5 days. At 24 hpf, the location of the yolk inclusion was scored according to the location along the body plan as: head region (anterior to the posterior end of the otic vesicle), mid-section (from the otic vesicle to the posterior end of the yolk extension), or tail region (posterior to the end of the yolk extension). The presence of an inflated swim bladder was scored at 5 dpf as a sign of embryonic viability. Statistical analysis was performed using unpaired two-tailed Student's *t*-test.

Sequencing of maternal crispants to identify genetic lesions

Females that produced maternal crispant embryos were used for *in vitro* fertilization (IVF) modified for haploid production, using UV-irradiated sperm as previously described (Baars et al., 2016). During maternal crispant haploid production, to minimize in adult females side-effects associated with the modified IVF procedure, the F0 adult females were manipulated as little as possible (ideally only once), and all resulting maternal crispant haploid embryos, which varied in fraction within the clutch and number,

Development (2021) 148, dev199536. doi:10.1242/dev.199536

were sequenced. Briefly, the night before the IVF procedure, single F0 adult females were placed into mating boxes together with single wild-type AB males, with a physical barrier separating males and females. On the morning of the IVF procedure, the barrier was removed, allowing natural mating. Tanks were monitored, and the F0 females were separated immediately after the first signs of egg release. In the same morning, a sperm solution was prepared using wild-type testes macerated in Hanks' solution (corresponding to testes from one male per 100 µl of Hanks'), disseminating sperm into solution, with the solution then UV-treated for 90 s to inactivate its DNA. Separated F0 females were anesthetized with tricaine solution (2% buffered tricaine in 100 ml of conditioned fish water), and mature eggs were extruded by applying gentle pressure to the abdomen. The extruded eggs were fertilized by the addition of 100 µl of UV-treated sperm solution with gentle mixing, followed by water-activation through the addition of E3 embryonic medium (1 ml for the first minute and flooding of the plate after the first minute). The resulting maternal haploid embryos were allowed to develop for 6-8 h, with the time period augmenting DNA content through DNA replication in the developing embryos. After 6-8 h, DNA was extracted from embryos that displayed a maternal crispant phenotype as previously described (Meeker et al., 2007), except that we used half of the volume (50 µl of 20 mM NaOH and 5 µl of Tris-HCl pH 8.0) compared with the original protocol in order to concentrate the DNA.

To analyze genetic lesions in maternal haploids, DNA fragments corresponding to the targeted genes were PCR amplified using genomic DNA extracts from single haploid embryos. The PCR primers were designed to include multiple guide sites in order to capture potential site-spanning indels (Table S2). Duplicate PCR reactions of each sample were carried out, and the amplified products were pooled using a DNA Clean and Concentrator kit (Zymo Research). The resulting amplified fragments were analyzed by Sanger sequencing using forward and reverse sequencing primers (Table S2). Sequence results were analyzed using Sequencher.

Acknowledgements

We thank past and current members of the Pelegri lab for their contributions to our research, particularly our animal husbandry staff for the care of the aquatic facility. We are also grateful for the comments and insight on the manuscript by Christina Hansen and Ryan Trevena. Microscopy was performed at the Newcomb Imaging Center, Department of Botany at the University of Wisconsin-Madison.

Competing interests

The authors declare no competing or financial interests.

Author contributions

Conceptualization: C.E.M., F.P.; Methodology: C.E.M.; Validation: C.E.M., G.C.V.; Formal analysis: C.E.M.; Investigation: C.E.M., G.C.V., J.O.; Writing - original draft: C.E.M.; Writing - review & editing: C.E.M., G.C.V., F.P.; Visualization: C.E.M.; Supervision: C.E.M., F.P.; Funding acquisition: F.P.

Funding

This work was funded by a grant from the National Institutes of Health (GM065303 to F.P.). Deposited in PMC for release after 12 months.

Peer review history

The peer review history is available online at https://journals.biologists.com/dev/article-lookup/doi/10.1242/dev.199536

References

Aanes, H., Winata, C. L., Lin, C. H., Chen, J. P., Srinivasan, K. G., Lee, S. G. P., Lim, A. Y. M., Hajan, H. S., Collas, P., Bourque, G. et al. (2011). Zebrafish mRNA sequencing deciphers novelties in transcriptome dynamics during maternal to zygotic transition. *Genome Res.* **21**, 1328-1338. doi:10.1101/gr.116012.110

Abrams, E. W. and Mullins, M. C. (2009). Early zebrafish development: it's in the maternal genes. *Curr. Opin. Genet. Dev.* **19**, 396-403. doi:10.1016/j.gde.2009.06.002

Aken, B. L., Ayling, S., Barrell, D., Clarke, L., Curwen, V., Fairley, S., Fernandez Banet, J., Billis, K., García Girón, C., Hourlier, T. et al. (2016). The Ensembl gene annotation system. *Database (Oxford)* **2016**, 1-19.

Allen, F., Crepaldi, L., Alsinet, C., Strong, A. J., Kleshchevnikov, V., De Angeli, P., Páleníková, P., Khodak, A., Kiselev, V., Kosicki, M. et al. (2018). Predicting the mutations generated by repair of Cas9-induced double-strand breaks. *Nat. Biotechnol.* **37**, 64-72. doi:10.1038/nbt.4317

Baars, D. L., Takle, K. A., Heier, J. and Pelegri, F. (2016). Ploidy manipulation of zebrafish embryos with Heat Shock 2 TREATMENT. *J Vis Exp.* **118**. doi:10.3791/54492

Boroviak, T., Stirparo, G. G., Dietmann, S., Hernando-Herraez, I., Mohammed, H., Reik, W., Smith, A., Sasaki, E., Nichols, J. and Bertone, P. (2018). Single cell transcriptome analysis of human, marmoset and mouse embryos reveals common and divergent features of preimplantation development. *Development* **145**, dev167833. doi:10.1242/dev.167833

Bradley, A. O., Vizcarra, C. L., Bailey, H. M. and Quinlan, M. E. (2020). Spire stimulates nucleation by Cappuccino and binds both ends of actin filaments. *Mol. Biol. Cell* **31**, 273-286. doi:10.1091/mbc.E19-09-0550

Brand, M., Granato, M., Nüsslein-Volhard, C., Nusslein-Volhard, C. and Dahm, R. (2002). Zebrafish: A practical approach. *Keeping and Raising Zebrafish* **7**, 39.

Breitsprecher, D. and Goode, B. L. (2013). Formins at a glance. *J. Cell Sci.* **126**, 1-7. doi:10.1242/jcs.107250

Brunner, E., Yagi, R., Debrunner, M., Beck-Schneider, D., Burger, A., Escher, E., Mosimann, C., Hausmann, G. and Basler, K. (2019). CRISPR-induced double-strand breaks trigger recombination between homologous chromosome arms. *Life Science Alliance* **2**, e201800267. doi:10.26508/lsa.201800267

Burger, A., Lindsay, H., Felker, A., Hess, C., Anders, C., Chiavacci, E., Zaugg, J., Weber, L. M., Catena, R., Jinek, M. et al. (2016). Maximizing mutagenesis with solubilized CRISPR-Cas9 ribonucleoprotein complexes. *Development* **143**, 2025-2037.

Campbell, P. D. and Updike, D. L. (2015). CSR-1 and P granules suppress sperm-specific transcription in the C. elegans germline. *Development* **142**, 1745-1755. doi:10.1242/dev.121434

Conti, E., Uy, M., Leighton, L., Blobel, G. and Kuriyan, J. (1998). Crystallographic analysis of the recognition of a nuclear localization signal by the nuclear import factor karyopherin α. *Cell* **94**, 193-204. doi:10.1016/S0092-8674(00)81419-1

Dosch, R. (2014). Next generation mothers: maternal control of germline development in zebrafish. *Crit. Rev. Biochem. Mol. Biol.* **50**, 54-68. doi:10.3109/10409238.2014.985816

Doyon, Y., McCammon, J. M., Miller, J. C., Faraji, F., Ngo, C., Katibah, G. E., Amora, R., Hocking, T. D., Zhang, L., Rebar, E. J. et al. (2008). Heritable targeted gene disruption in zebrafish using designed zinc-finger nucleases. *Nat. Biotechnol.* **26**, 702-708. doi:10.1038/nbt1409

Eno, C. and Pelegri, F. (2018). Modulation of F-actin dynamics by maternal Mid1ip1L controls germ plasm aggregation and furrow recruitment in the zebrafish embryo. *Development* **145**, dev156596. doi:10.1242/dev.156596

Eno, C., Solanki, B. and Pelegri, F. (2016). Aura (mid1ip1l) regulates the cytoskeleton at the zebrafish egg-to-embryo transition. *Development* **143**, 1585-1599.

Fuentes, R. and Fernández, J. (2010). Ooplasmic segregation in the zebrafish zygote and early embryo: Pattern of ooplasmic movements and transport pathways. *Dev. Dyn.* **239**, 2172-2189. doi:10.1002/dvdy.22349

Gagnon, J. A., Valen, E., Thyme, S. B., Huang, P., Ahkmetova, L., Pauli, A., Montague, T. G., Zimmerman, S., Richter, C. and Schier, A. F. (2014). Efficient Mutagenesis by Cas9 protein-mediated oligonucleotide insertion and large-scale assessment of single-guide RNAs. *PLoS One* **9**, e98186. doi:10.1371/journal.pone.0098186

Ge, X., Grotjahn, D., Welch, E., Lyman-Gingerich, J., Holguin, C., Dimitrova, E., Abrams, E. W., Gupta, T., Marlow, F. L., Yabe, T. et al. (2014). Hecate/Grip2a acts to reorganize the cytoskeleton in the symmetry-breaking event of embryonic axis induction. *PLoS Genet.* **10**, e1004422. doi:10.1371/journal.pgen.1004422

Goode, B. L. and Eck, M. J. (2007). Mechanism and function of formins in the control of actin assembly. *Annu. Rev. Biochem.* **76**, 593-627. doi:10.1146/annurev.biochem.75.103004.142647

Görlich, D., Prehn, S., Laskey, R. A. and Hartmann, E. (1994). Isolation of a protein that is essential for the first step of nuclear protein import. *Cell* **79**, 767-778. doi:10.1016/0092-8674(94)90067-1

He, W.-X., Wu, M., Liu, Z., Li, Z., Wang, Y., Zhou, J., Yu, P., Zhang, X.-J., Zhou, L. and Gui, J.-F. (2018). Oocyte-specific maternal Slbp2 is required for replication-dependent histone storage and early nuclear cleavage in zebrafish oogenesis and embryogenesis. *RNA* **24**, 1738-1748. doi:10.1261/rna.067090.118

Hegsted, A., Yingling, C. V. and Pruyne, D. (2017). Inverted formins: A subfamily of atypical formins. *Cytoskeleton (Hoboken)* **74**, 405-419. doi:10.1002/cm.21409

Higgs, H. N. and Peterson, K. J. (2005). Phylogenetic analysis of the formin homology 2 domain. *Mol. Biol. Cell* **16**, 1-13. doi:10.1091/mbc.e04-07-0565

Hu, J., Wang, F., Yuan, Y., Zhu, X., Wang, Y., Zhang, Y., Kou, Z., Wang, S. and Gao, S. (2010). Novel importin-alpha family member Kpna7 is required for normal fertility and fecundity in the mouse. *J. Biol. Chem.* **285**, 33113-33122. doi:10.1074/jbc.M110.117044

Huang, P., Xiao, A., Zhou, M., Zhu, Z., Lin, S. and Zhang, B. (2011). Heritable gene targeting in zebrafish using customized TALENs. *Nat. Biotechnol.* **29**, 699-700. doi:10.1038/nbt.1939

Hwang, W. Y., Fu, Y., Reyon, D., Maeder, M. L., Tsai, S. Q., Sander, J. D., Peterson, R. T., Yeh, J.-R. J. and Joung, J. K. (2013). Efficient genome editing in zebrafish using a CRISPR-Cas system. *Nat. Biotechnol.* **31**, 227-229. doi:10.1038/nbt.2501

Imamoto, N., Tachibana, T., Matsubae, M. and Yoneda, Y. (1995). A karyophilic protein forms a stable complex with cytoplasmic components prior to nuclear pore binding. *J. Biol. Chem.* **270**, 8559-8565. doi:10.1074/jbc.270.15.8559

Jao, L.-E., Wente, S. R. and Chen, W. (2013). Efficient multiplex biallelic zebrafish genome editing using a CRISPR nuclease system. *Proc. Natl. Acad. Sci. USA* **110**, 13904-13909. doi:10.1073/pnas.1308335110

Kane, D. A., Hammerschmidt, M., Mullins, M. C., Maischein, H. M., Brand, M., van Eeden, F. J., Furutani-Seiki, M., Granato, M., Haffter, P., Heisenberg, C. P. et al. (1996). The zebrafish epiboly mutants. *Development* **123**, 47-55. doi:10.1242/dev.123.1.47

Kelley, J. B., Talley, A. M., Spencer, A., Gioeli, D. and Paschal, B. M. (2010). Karyopherin alpha7 (KPNA7), a divergent member of the importin alpha family of nuclear import receptors. *BMC Cell Biol.* **11**, 63. doi:10.1186/1471-2121-11-63

Kimmel, C. B., Ballard, W. W., Kimmel, S. R., Ullmann, B. and Schilling, T. F. (1995). Stages of embryonic development of the zebrafish. *Dev. Dyn.* **203**, 253-310. doi:10.1002/aja.1002030302

Knaut, H., Pelegri, F., Bohmann, K., Schwarz, H. and Nüsslein-Volhard, C. (2000). Zebrafish vasa RNA but not its protein is a component of the germ plasm and segregates asymmetrically before germline specification. *J. Cell Biol.* **149**, 875-888. doi:10.1083/jcb.149.4.875

Labun, K., Montague, T. G., Gagnon, J. A., Thyme, S. B. and Valen, E. (2016). CHOPCHOP v2: a web tool for the next generation of CRISPR genome engineering. *Nucleic Acids Res.* **44**, W272-W276. doi:10.1093/nar/gkw398

Leader, B., Lim, H., Carabatsos, M. J., Harrington, A., Ecsedy, J., Pellman, D., Maas, R. and Leder, P. (2002). Formin-2, polyploidy, hypofertility and positioning of the meiotic spindle in mouse oocytes. *Nat. Cell Biol.* **4**, 921-928. doi:10.1038/ncb880

Lee, M. T., Bonneau, A. R., Takacs, C. M., Bazzini, A. A., DiVito, K. R., Fleming, E. S. and Giraldez, A. J. (2013). Nanog, Pou5f1 and SoxB1 activate zygotic gene expression during the maternal-to-zygotic transition. *Nature* **503**, 360-364. doi:10.1038/nature12632

Leung, C. F., Webb, S. E. and Miller, A. L. (2000). On the mechanism of ooplasmic segregation in single-cell zebrafish embryos. *Dev. Growth Differ.* **42**, 29-40. doi:10.1046/j.1440-169x.2000.00484.x

Lindeman, R. E. and Pelegri, F. (2012). Localized products of futile cycle/lrmp promote centrosome-nucleus attachment in the zebrafish zygote. *Curr. Biol.* **22**, 843-851. doi:10.1016/j.cub.2012.03.058

Long, M., Betrán, E., Thornton, K. and Wang, W. (2003). The origin of new genes: glimpses from the young and old. *Nat. Rev. Genet.* **4**, 865-875. doi:10.1038/nrg1204

Lu, J., Peatman, E., Tang, H., Lewis, J. and Liu, Z. (2012). Profiling of gene duplication patterns of sequenced teleost genomes: evidence for rapid lineage-specific genome expansion mediated by recent tandem duplications. *BMC Genomics* **13**, 246.

Lynch, M. and Conery, J. S. (2000). The evolutionary fate and consequences of duplicate genes. *Science* **290**, 1151-1155. doi:10.1126/science.290.5494.1151

Manseau, L. J. and Schüpbach, T. (1989). Cappuccino and spire: two unique maternal-effect loci required for both the anteroposterior and dorsoventral patterns of the Drosophila embryo. *Genes Dev.* **3**, 1437-1452. doi:10.1101/gad.3.9.1437

Meeker, N. D., Hutchinson, S. A., Ho, L. and Trede, N. S. (2007). Method for isolation of PCR-ready genomic DNA from zebrafish tissues. *BioTechniques* **43**, 610-614.

Meng, X., Noyes, M. B., Zhu, L. J., Lawson, N. D. and Wolfe, S. A. (2008). Targeted gene inactivation in zebrafish using engineered zinc-finger nucleases. *Nat. Biotechnol.* **26**, 695-701. doi:10.1038/nbt1398

Meyer, A. and Schartl, M. (1999). Gene and genome duplications in vertebrates: the one-to-four (-to-eight in fish) rule and the evolution of novel gene functions. *Curr. Opin. Cell Biol.* **11**, 699-704. doi:10.1016/S0955-0674(99)00039-3

Montague, T. G., Cruz, J. M., Gagnon, J. A., Church, G. M. and Valen, E. (2014). CHOPCHOP: a CRISPR/Cas9 and TALEN web tool for genome editing. *Nucleic Acids Res.* **42**, W401-W407. doi:10.1093/nar/gku410

Moravec, C. E. and Pelegri, F. J. (2019). An accessible protocol for the generation of CRISPR-Cas9 knockouts using INDELs in Zebrafish. *Methods Mol. Biol.* **1920**, 377-392. doi:10.1007/978-1-4939-9009-2_23

Moravec, C. E., Samuel, J., Weng, W., Wood, I. C. and Sirotkin, H. I. (2016). Maternal Rest/Nrsf regulates Zebrafish behavior through snap25a/b. *J. Neurosci.* **36**, 9407-9419. doi:10.1523/JNEUROSCI.1246-16.2016

Moreno-Mateos, M. A., Vejnar, C. E., Beaudoin, J.-D., Fernandez, J. P., Mis, E. K., Khokha, M. K. and Giraldez, A. J. (2015). CRISPRscan: designing highly efficient sgRNAs for CRISPR-Cas9 targeting in vivo. *Nat. Methods* **12**, 982-988. doi:10.1038/nmeth.3543

Moroianu, J., Blobel, G. and Radu, A. (1995). Previously identified protein of uncertain function is karyopherin alpha and together with karyopherin beta docks import substrate at nuclear pore complexes. *Proc. Natl. Acad. Sci. USA* **92**, 2008-2011. doi:10.1073/pnas.92.6.2008

Nair, S., Marlow, F., Abrams, E., Kapp, L., Mullins, M. C. and Pelegri, F. (2013). The chromosomal passenger protein Birc5b organizes microfilaments and germ plasm in the Zebrafish embryo. *PLoS Genet.* **9**, e1003448. doi:10.1371/journal.pgen.1003448

Nair, S., Welch, E. L., Moravec, C. E., Trevena, R. L. and Pelegri, F. (2021). A midbody component homolog, too much information/prc1-like, is required for microtubule reorganization during both cytokinesis and axis induction in the early zebrafish embryo. *bioRxiv* 2021.06.10.447958.

Ohno, S. (2013). *Evolution by Gene Duplication*. Berlin, Heidelberg: Springer Berlin/Heidelberg.

Pfender, S., Kuznetsov, V., Pleiser, S., Kerkhoff, E. and Schuh, M. (2011). Spire-type actin nucleators cooperate with Formin-2 to drive asymmetric oocyte division. *Curr. Biol.* **21**, 955-960. doi:10.1016/j.cub.2011.04.029

Sandve, S. R., Rohlfs, R. V. and Hvidsten, T. R. (2018). Subfunctionalization versus neofunctionalization after whole-genome duplication. *Nat. Genet.* **50**, 908-909. doi:10.1038/s41588-018-0162-4

Shah, A. N., Davey, C. F., Whitebirch, A. C., Miller, A. C. and Moens, C. B. (2015). Rapid reverse genetic screening using CRISPR in zebrafish. *Nat. Methods* **12**, 535-540. doi:10.1038/nmeth.3360

Shankaran, S. S., Dahlem, T. J., Bisgrove, B. W., Yost, H. J. and Tristani–Firouzi, M. (2017). CRISPR/Cas9-directed gene editing for the generation of loss-of-function mutants in high-throughput Zebrafish F_0 screens. *Curr. Protoc. Mol. Biol.* **119**, 31.9.1-31.9.22. doi:10.1002/cpmb.42

Tejomurtula, J., Lee, K.-B., Tripurani, S. K., Smith, G. W. and Yao, J. (2009). Role of importin alpha8, a new member of the importin alpha family of nuclear transport proteins, in early embryonic development in cattle. *Biol. Reprod.* **81**, 333-342. doi:10.1095/biolreprod.109.077396

Trubiroha, A., Gillotay, P., Giusti, N., Gacquer, D., Libert, F., Lefort, A., Haerlingen, B., De Deken, X., Opitz, R. and Costagliola, S. (2018). A rapid CRISPR/Cas-based Mutagenesis assay in Zebrafish for identification of genes involved in thyroid morphogenesis and function. *Sci. Rep.* **8**, 5647. doi:10.1038/s41598-018-24036-4

Vuorinen, E. M., Rajala, N. K., Ihalainen, T. O. and Kallioniemi, A. (2018). Depletion of nuclear import protein karyopherin alpha 7 (KPNA7) induces mitotic defects and deformation of nuclei in cancer cells. *BMC Cancer* **18**, 325. doi:10.1186/s12885-018-4261-5

Walker, C. (1998). Chapter 3 Haploid Screens and Gamma-Ray Mutagenesis. In *Methods in Cell Biology* (ed. H.W. Detrich, M. Westerfield and L.I. Zon), pp. 43-70. Academic Press.

Wang, X., Park, K.-E., Koser, S., Liu, S., Magnani, L. and Cabot, R. A. (2012). KPNA7, an oocyte- and embryo-specific karyopherin α subtype, is required for porcine embryo development. *Reprod. Fertil. Dev.* **24**, 382-391. doi:10.1071/RD11119

White, R. J., Collins, J. E., Sealy, I. M., Wali, N., Dooley, C. M., Digby, Z., Stemple, D. L., Murphy, D. N., Billis, K., Hourlier, T. et al. (2017). A high-resolution mRNA expression time course of embryonic development in zebrafish. *Elife* **6**, e30860. doi:10.7554/eLife.30860

Wu, R. S., Lam, I. I., Clay, H., Duong, D. N., Deo, R. C. and Coughlin, S. R. (2018). A rapid method for directed gene knockout for screening in G0 Zebrafish. *Dev. Cell* **46**, 112-125.e4. doi:10.1016/j.devcel.2018.06.003

Wühr, M., Tan, E. S., Parker, S. K., Detrich, H. W. and Mitchison, T. J. (2010). A model for cleavage plane determination in early amphibian and fish embryos. *Curr. Biol.* **20**, 2040-2045. doi:10.1016/j.cub.2010.10.024

Yasuhara, N., Takeda, E., Inoue, H., Kotera, I. and Yoneda, Y. (2004). Importin α/β-mediated nuclear protein import is regulated in a cell cycle-dependent manner. *Exp. Cell Res.* **297**, 285-293. doi:10.1016/j.yexcr.2004.03.010

Young, K. G., Thurston, S. F., Copeland, S., Smallwood, C. and Copeland, J. W. (2008). INF1 is a novel microtubule-associated formin. *Mol. Biol. Cell* **19**, 5168-5180. doi:10.1091/mbc.e08-05-0469

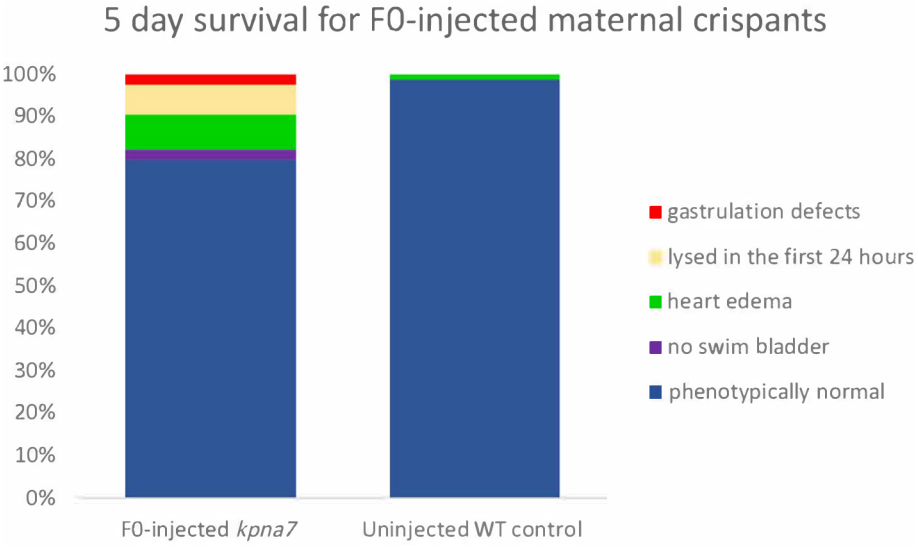

Fig. S1. Injection of multiple guide RNAs into one-cell embryos has a minimal effect on viability compared to uninjected controls, as scored by the presence of a swim bladder at five days.

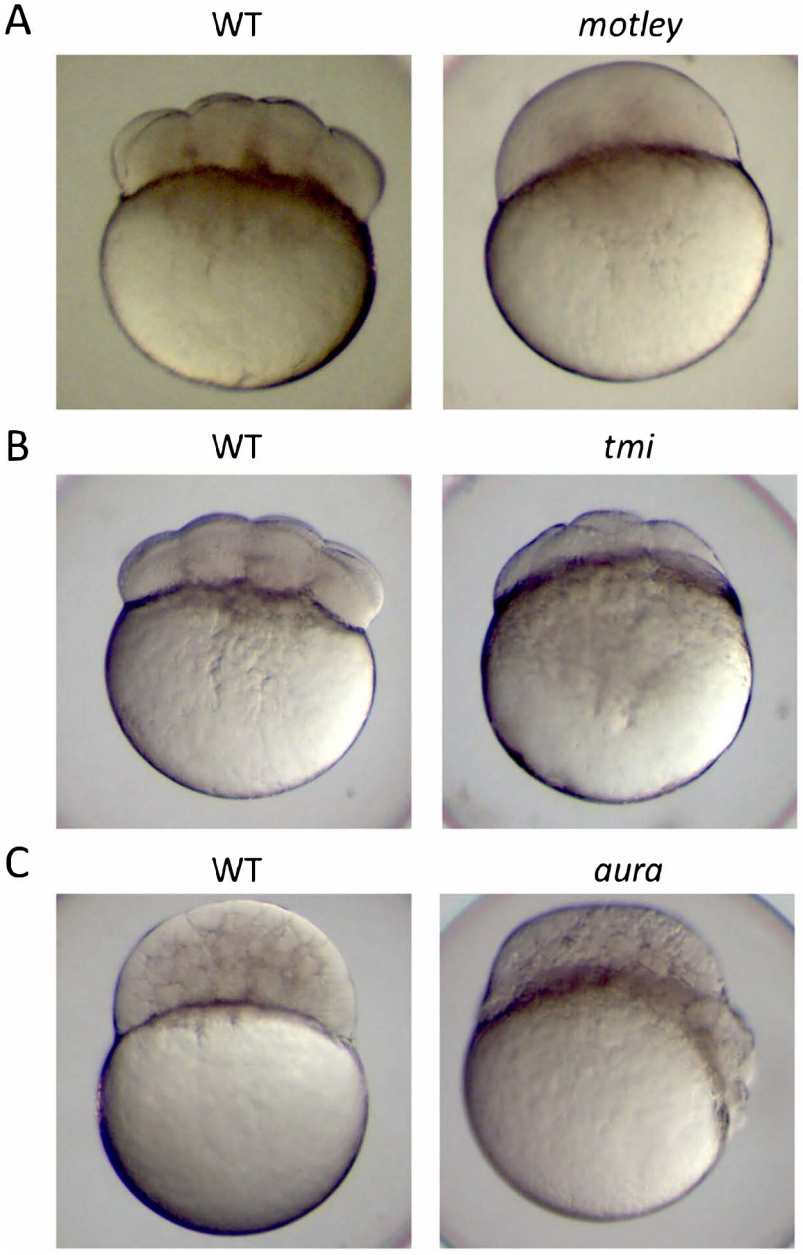

Fig. S2. Representative images of known maternal-effect mutants: *motley* (A), *too much information* (*tmi*) (B), and *aura* (C).

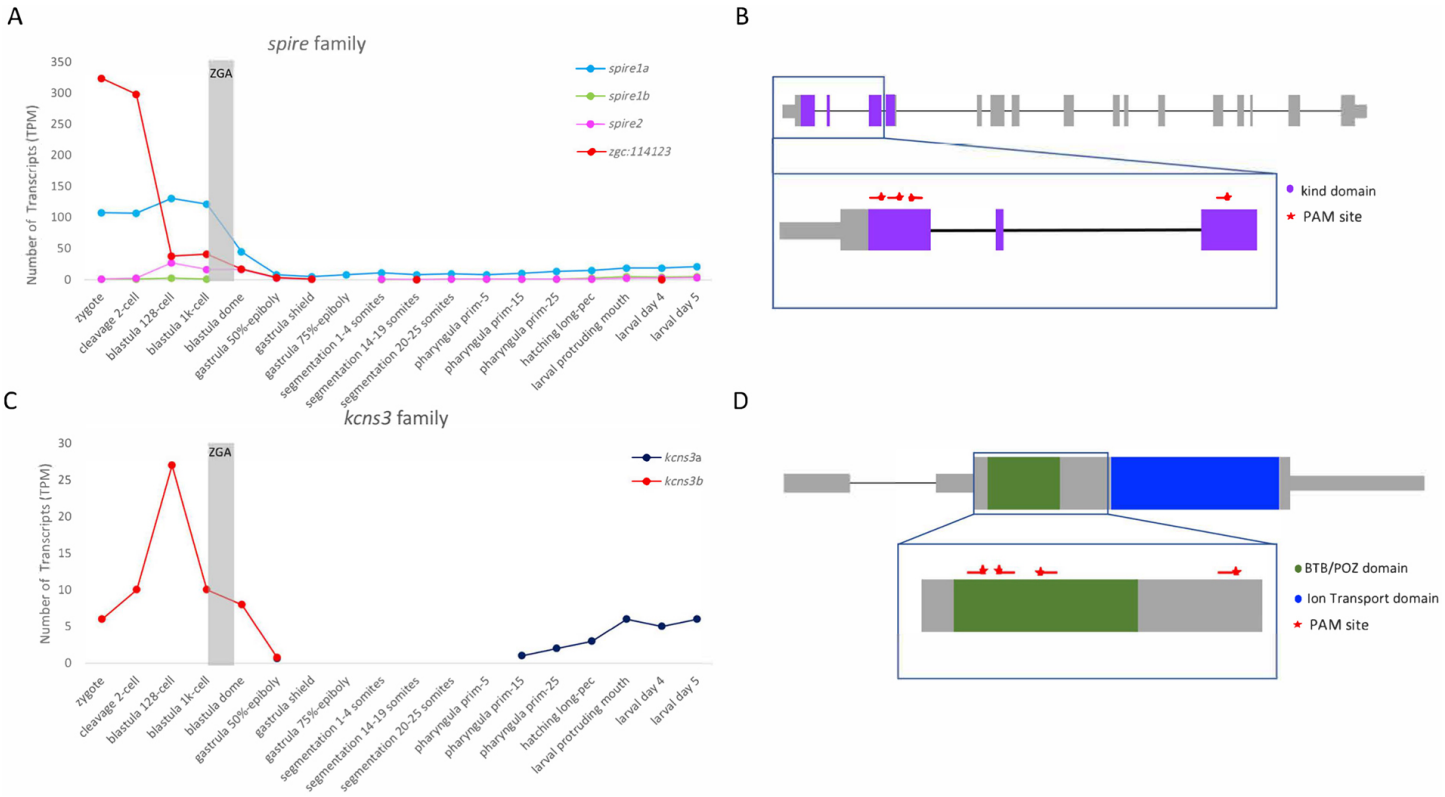

Fig. S3. mRNA expression levels and gene structures for candidate maternal-effect genes, *zgc:114123* and *kcns3b*, did not display a phenotype in the maternal crispants. A, C) Expression pattern for the *spire* (A) and *kcns3*(C) families during early development, from zygote to larval day 5. Expression of maternal-specific transcripts for each family is represented in red, and the gray bar marks zygotic genome activation. (B, D) Gene structure diagrams of *zgc:114123* (B) and *kcns3b* (D), with guide RNA target sites (red lines) and PAM sites (red stars).

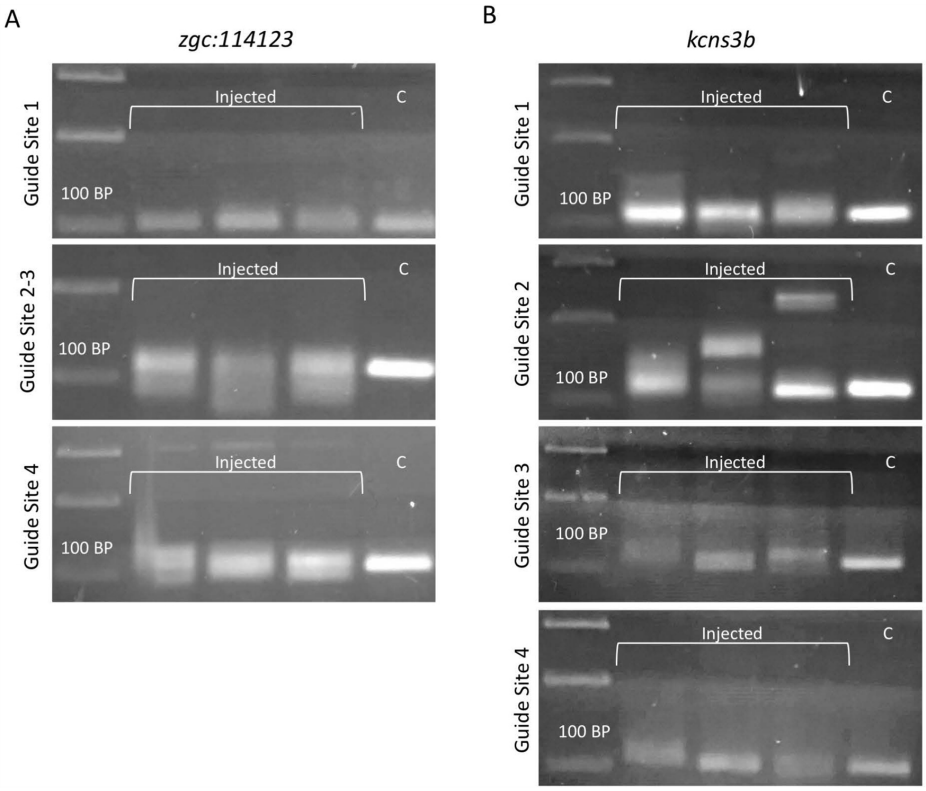

Fig. S4. INDELS found in the somatic tissue of F0-injected embryos at 24 hpf for *zgc:114123*(A) and *kcns3b* (B).

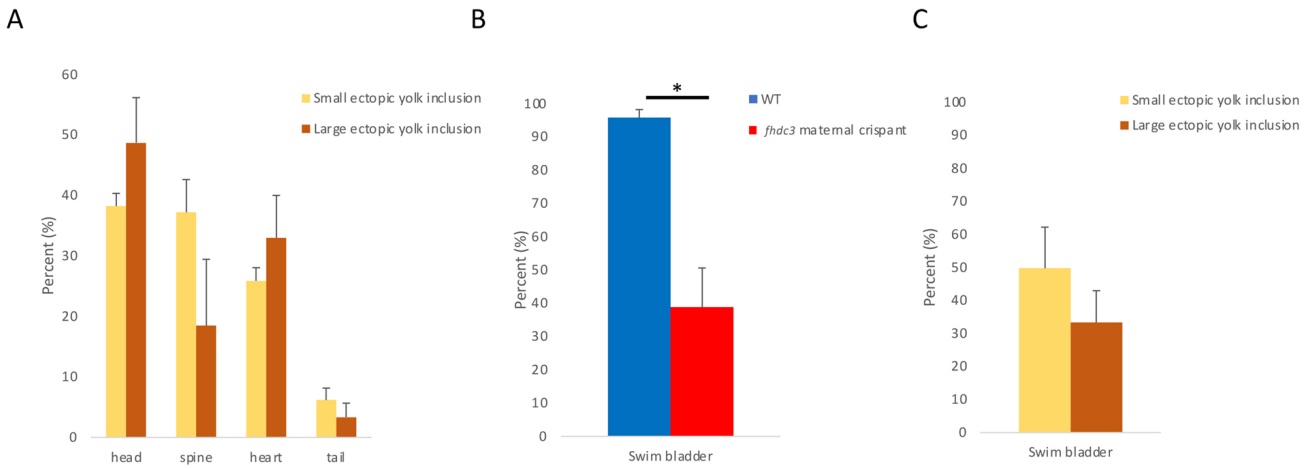

Fig. S5. Viability of the *fhdc3* maternal crispant embryos is not influenced by the amount of ectopic yolk in the embryo. A) In *fhdc3* maternal crispant embryos, there is no difference in the location of the yolk at one day between large and small ectopic yolk inclusions. B) *fhdc3* maternal crispant embryos have decreased viability when compared to wild-type controls as scored by the presence of the swim bladder at 5 days (P-value =.0091). C) No difference was observed when comparing the size of yolk and viability in the *fhdc3* maternal crispant embryos, as scored by the presences of the swim bladder at 5 days (swim bladder inflation (> 1/8 of blastodisc volume: 34%, n=54; < 1/8 of blastodisc volume: 45%, n=57; P-value = 0.4235).

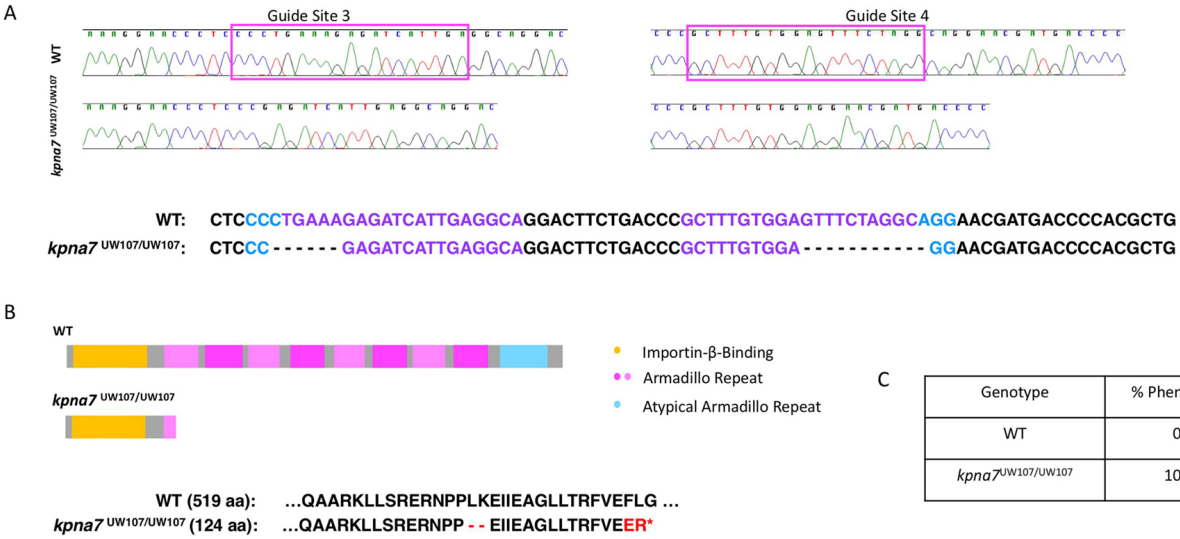

Genotype	% Phenotype	N
WT	0	238
kpna7$^{UW107/UW107}$	100	365

Fig. S6. Validation of the *kpna7* maternal crispant phenotype using a stable Crispr-Cas9 line. A) Chromatograms and sequencing alignments for wild-type and *kpna7*$^{UW107/UW107}$ samples lesions in edited guide sites. In the sequencing alignment, the purple text represents the guide sites, and the blue text is the PAM site. B) Diagrams highlighting known conserved domains in the Kpna7 protein and the predicted truncated product encoded by the *kpna7*^{UW107} allele and amino acid sequences showing the predicted changes and appearance of a premature stop codon. C) Embryos from *kpna7*$^{UW107/UW107}$ females exhibit a fully penetrant phenotype identical to that observed in *kpna7* maternal crispants.

Table S1. candidate genes *zgc:114123* and *kcns3b* did not result in any apparent maternal crispant embryos.

Gene	Fish	Number of embryos in F1 generation	% Phenotype (gross morphological changes)
zgc:114123	WT	63	0
	1	78	0
	2	63	0
kcns3b	WT	92	0
	1	136	0
	2	62	0
	3	51	0

Table S2. List of DNA oligos for guide RNAs and primers used in this study.

Click here to download Table S2

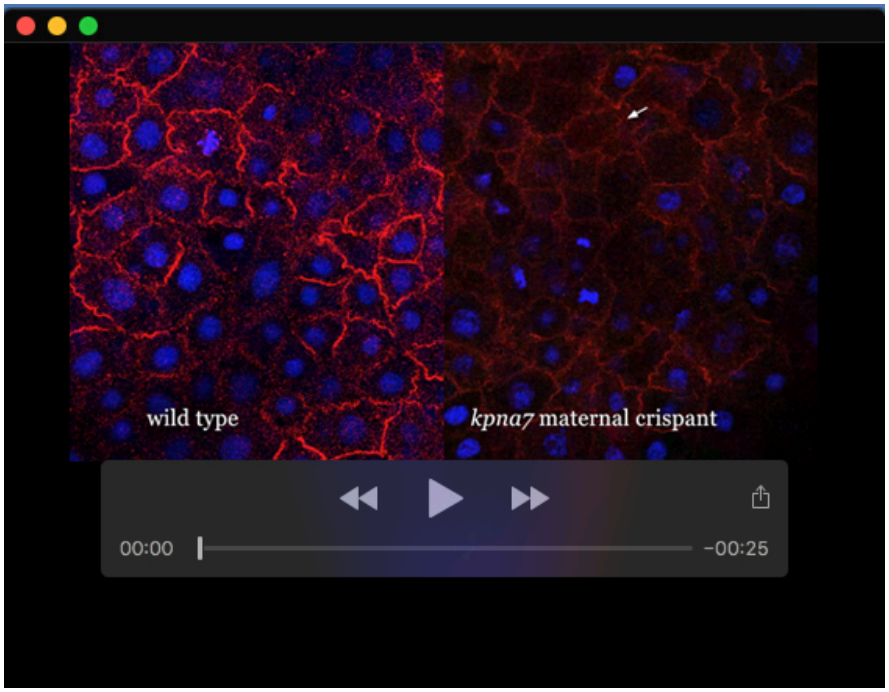

Movie 1. Cellular cortex of a *kpna7* maternal crispant and wild-type embryo at 6 hpf. Individual focal planes of confocal *Z*-stack of a 6 hpf embryo (shown as a 2D *Z*-projection in Figure 4B). The cell membranes are labeled with anti-β-catenin antibodies (red) and DNA is stained with DAPI (blue). Visualization of sequential focal planes demonstrates that the *kpna7* maternal crispants contain cells that lack nuclei.